ELASTO-PLASTIC TORSION WITH WORK-HARDENING

BY

PRAKASH CHANDRA UPADHYAYA

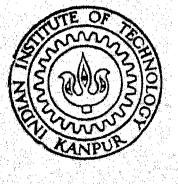

DEPARTMENT OF MECHANICAL ENGINEERING

INDIAN INSTITUTE OF TECHNOLOGY KANPUR

JULY, 1970

ELASTO - PLASTIC TORSION

WITH WORK-HARDENING

A Thesis Submitted
In Partial Fulfilment of the Requirements
for the Degree of

MASTER OF TECHNOLOGY

By

PRAKASH CHANDRA UPADHYAYA

to the

DEPARTMENT OF MECHANICAL ENGINEERING
INDIAN INSTITUTE OF TECHNOLOGY, KANPUR

July, 1970

CERTIFICATE

This is to certify that this work has been carried out under my supervision and has not been submitted for a degree elsewhere.

(Dr. V.K. Stokes)
Associate Professor
Dept. of Mechanical Engineering
Indian Institute of Technology,
Kanpur

ACKNOWLEDGEMENT

It is my pleasure and privilege to express my deep sense of gratitude to Prof. V.K. Stokes for initiating me into this area of research and for his invaluable guidance and constant encouragement during the course of this work.

I wish to thank the staff of the Computer Centre, I.I.T. Kanpur for their help and cooperation in carrying out the computational work.

I also wish to express my thanks to Shri J.D. Varma for the pains he has taken in typing this work and Shri Lallu Singh who did the fine job of cyclostyling.

P.C. UPADHYAYA

TABLE OF CONTENTS

LIST OF FIGURES

NOMENCLATURE

T = Twisting moment or torque

T_o = Twisting moment just sufficient to start yielding.

u = Displacement in the x - direction.

v = Displacement in the y - direction.

w = Displacement in the z - direction.

$\sigma_i = \sigma_{ii}$ = Normal stress on the face whose normal is in the i - direction.

τ_{ij} = Shear stress in the j - direction acting on a face whose normal is in i -direction.

S_{ij} = Deviatoric stress.

$\epsilon_i = \epsilon_{ii}$ = Normal strain on the face whose normal is in the i - direction.

γ_{ij} = Shear strain in the j - direction acting on a face whose normal is in the i - direction.

G = Modulus of rigidity.

E = Modulus of elasticity.

ν = Poisson's ratio.

ψ, Φ = Stress function.

∇^2 = Laplacian operator.

K = Yield shear stress.

Γ = Boundary of a region.

θ_0 = Angle of twist per unit length just sufficient to start yielding at a point.

q = Resultant shear stress.

σ_Y , σ_0 = Yield stress in simple tension.

ϵ_0 , ϵ_Y = Yield strain in simple tension.

$\bar{\epsilon}_{ij}$ = Strain normalized with respect to ϵ_Y

$\bar{\tau}_{ij}$ = Stress non-dimensionalized with respect to σ_Y.

α = Permanent plastic strain required for yielding to start.

n = Strain hardening coefficient.

E' = Slope beyond the yield point, for a piecewise linear stress-strain curve.

$\lambda = \frac{3}{2}\left(\frac{E}{E'} - 1\right)$ = Strain hardening parameter for piecewise linear stress-strain relation.

$\bar{\sigma}_e$, χ = Effective stress (in our case it is resultant shear stress non-dimensionalized with respect to the yield stress).

ξ , η = Non-dimensional distance variables.

Φ_x = First partial derivative of Φ with respect to x.

Φ_y = First partial derivative of Φ with respect to y.

Φ_{xx} = Second partial derivative of Φ with respect to x.

Φ_{yy} = Second partial derivative of Φ with respect to y.

L = A characteristic length of the cross-section.

h = Mesh size.

ELASTOPLASTIC TORSION WITH WORK HARDENING

A Thesis submitted
In Partial Fulfilment of the Requirements,
For the Degree of
MASTER OF TECHNOLOGY IN MECHANICAL ENGINEERING
by

P. C. UPADHYAYA
to the
Department of Mechanical Engineering,
INDIAN INSTITUTE OF TECHNOLOGY, KANPUR
July, 1970

ABSTRACT

In this thesis a numerical technique for solving the elasto-plastic torsion problem for Ramberg - Osgood type of materials has been prepared. The deformation theory of plasticity has been used to take into account the work-hardening effect. The elastic and plastic torsion equations have been satisfied in their respective regions and the location of the elasto-plastic boundary has been determined.

Numerical results have been obtained for square, rectangular and thick L - shaped cross-sections. The effects of work-hardening on the elasto-plastic boundary and on the shear stress distribution over the cross - section, for different values of the angle of twist and the strain hardening parameter n, have been considered.

It has been shown that the elasto-plastic boundary is not appreciably affected by changes in the work hardening parameter n for low values of the angle of twist, but that the shear stress distribution inside the plastic region keeps changing with the strain hardening paremeter n. For large values of n (say 30 or more) solution approaches that for the elastic - ideally plastic case.

1. INTRODUCTION

1.1 NATURE OF ELASTO-PLASTIC PROBLEMS

In designing a structural member or a machine part, the engineer as a rule uses formulae which are based on the theory of elasticity. The highest stress predicted by these formulae is then compared with the maximum stress which the material can stand without failure. A factor of safety is derived from this comparision. Now, in all but the very simplest cases the factor of safety obtained in this manner will differ considerably from the factor of safety defined as the ratio of the ultimate load to the design load. The reason for this is the fact that, the stresses set up by the ultimate load will exceed the elastic limit of the material; so that the theory of elasticity is unable to predict these stresses. In order to obtain the second factor of safety, the only one with a physical meaning, the mechanical behaviour of the material beyond the elastic limit must be taken into account. It is here only that the theory of plasticity plays an important role.

For most of materials it is not possible to describe the entire stress - strain curve by means of a simple mathematical expression; so that in a given problem the behaviour of the material has to be approximated by an idealized stress-strain curve, which emphasizes those aspects of the behaviour which are of importance in that particular problem. Some idealized models of material behaviour are described by rigid, elastic, perfectly plastic, rigid plastic, elastic perfectly plastic and elastic-plastic (strain hardening) materials. These idealizations are useful for design work when the deformations are small and for carrying out detailed studies of the mechanism of fracture, wear and friction of ductile materials under different types of loading. In a deformed body, when a part of the body has yielded, elastic-plastic models of stress-strain curves are used for calculating the stresses and strains.

A complete solution of the general problem in plasticity involves a calculation of the stresses and the deformations in both, the elastic and plastic regions. In the former, the stress is directly connected with the total strain by means of Hooke's law. In the latter, there is no such correspondence and the stress-strain

differential relations have to be integrated by following the history of the deformation from the onset of plasticity at some point of the body. The process of plastic deformation has to be considered mathematically as a succession of small increments of strain, even when the over all distortion is so small that the change in external surfaces can be neglected. When the strains are large, the determination of the changing shape of the free plastic surface necessitates the consideration of the deformation from moment to moment.

The state of strain in a plastically deformed element of a strain hardening material may depend on the entire history to which the element has been subjected. However, for the particular type of stress history known as proportional loading, in which the components of the stress tensor increase in constant ratio to each other, the strains obviously can be expressed in terms of the final state of stress; for in this case the specification of the final state of stress also specifies the stress history. The deformation theories of plasticity, which relate the total plastic strain to the final stress, are therefore applicable to proportional loading.

The solutions in the elastic and plastic regions are inter-related by certain continuity conditions in the stress and displacements, which must be satisfied along the elastic-plastic boundary. This boundary is itself one of the unknowns in the problem and is usually of such an awkward shape that even the stress distribution in the elastic region can only be obtained by laborious numerical methods. The complete and accurate solution of a plastic problem can only be obtained in a relatively few cases.

1.2 REVIEW OF ELASTO-PLASTIC TORSION

So far, all the work on elasto-plastic torsion has been limited to the elastic ideally plastic case only. The effect of work hardening does not seem to have been considered by anyone. For an ideal plastic case (no work hardening) where the resultant shear stress at a point remains constant once it has yielded, an extension of the membrane analogy was first suggested by A. Nadai[1] (1923). This simulates the stress function for a partially plastic bar when the twist is so small that changes in the external contour can be neglected. Using this concept D.G. Christopherson[2] (1940), and D.G. Christopherson and R.V. Southwell[3] (1938) found

the elasto-plastic boundary for triangular and I-Sections by using relaxation methods. F.S. Shaw[4] (1944) calculated the stress and the elasto-plastic boundary for rectangular hollow sections. Sokolovsky[5] (1942) formulated an ingenious inverse method of solution for certain oval contours. His method consisted in assuming a mathematically convenient shape for the elastic-plastic boundary and determining from this the approximate contour of the section. But as Prof. R. Hill has pointed out, the success of Sokolovsky's method was due to the fact that the elastic-plastic boundary happens to be an ellipse. Moreover, this method can be applied only when the plastic region has developed all over the boundary. Sokolovsky[6] (1943), also investigated the plastic distribution of stress in a conical bar and in a stepped bar consisting of two cylinders of different radii; but did not calculate the plastic boundary or the displacements. Eddy and Shaw[7] (1949) applied relaxation methods to an approximate computation of the stress distribution and plastic boundary in a shaft with a collar. Apart from these, J.B. Walsh[8] (1957) studied the elasto-plastic torsion of a circumferentially notched bar and J.A.H.Hult[9] (1957) derived the shape of the incipient region at the tip of the sharp notch in a twisted bar. K.R. Rushton[10] (1963) developed an electrical analogue solution of

elastic-plastic torsion for shafts having discontinuties.

1.3 DESCRIPTION OF THE PROBLEM

As pointed out earlier, all the previous work was for elastic-ideally plastic materials only. However, most metals show a strain hardening effect when undergoing plastic deformation. This happens because after minor shear slips have occured, they show no further plastic strains untill higher stresses are applied. Therefore, it is necessary to consider work hardening while analysing a plastic or elasto-plastic problem.

To account for the work hardening effect, a deformation theory or flow theory of plasticity could be used. On theoretical grounds the flow theory is more sound. However, for small plastic deformations, the deformation theory also gives good results. Further, it has been shown by B. Budianskey[11] (1959) that the deformation theories of plasticity may be used for loading paths other than proportional loading, without violating the general requirements for the physical soundness of the theory of plasticity. The problem of plastic torsion was considered by J.H. HUTH[12] (1955). However, his results were inconclusive as they were based on a very coarse-mesh finite difference approximation. Later on, H.J. Greenberg[13] (1960) studied the comparision of flow

and deformation theories in the plastic torsion of a square section for the Ramberg Osgood[14] material. He established the validity of using the deformation theory in the torsion problem and the extent to which the predictions of the flow and deformation theories agree. Further, he justified the use of the deformation theory by showing that the criterion due to Budiansky[11] is satisfied. He also showed that for large values of n, the Ramberg Osgood[14] stress-strain law approaches the case of a perfect plastic material.

In this thesis a method for solving the elasto-plastic torsion problem for Ramberg-Osgood type of materials has been proposed, using the deformation theory of plasticity to take account of the strain-hardening effect. For the plastic region of the cross-section a seperate torsion equation has been derived, which comes out to be a non-linear partial differential equation. Owing to the non linearity involved, it is not possible to solve this equation analytically. Therefore, a numerical solution has been attempted using the finite difference technique. It is an iterative procedure, wherein the elastic-plastic boundary and the numerical values of the stress function keep on changing after each iteration and finally converge to a stable boundary. In the final

solution the plastic and elastic torsion equations are satisfied in their respective regions. Further the values of the stress function match at the common boundary and also satisfy the condition of continuity of the resultant shear stress.

The method has been tried for different types of cross-sections and for different values of the strain hardening parameter n.

Since the basic nature of the plastic torsion equation remains the same for the piecewise linear work hardening model, the technique has been used for solving the problem of the torsion of a square cross-section of a piecewise linear work-hardening material. The effects of the strain hardening parameter n on the elasto-plastic boundary and the resultant shearing stresses have been studied. The method has been tested for convergence to the elastic-ideally plastic solution by considering large values of n (say n = 30).

As the technique is based on the finite difference approximation, the effect of the mesh size has been studied from the point of view of computational time and convergence. This gives an approximate idea of the size of the mesh to be used for this method.

All the numerical results, which have been obtained to illustrate the working of the technique, are based on the approximate properties of steel. But the method could be used to study the behaviour of any other material in elasto-plastic torsion.

All the results were obtained on an I.B.M. 7044 Computer.

2. BASIC THEORY OF ELASTIC IDEALLY PLASTIC TORSION

The plastic analysis of prismatic bars in torsion can most usefully be approached by first considering simple elastic torsion; as the mathematical formulation of the problem of plastic torsion (with work hardening) is similar to the elastic case except that a different stress-strain relation is used and a few more assumptions are made. Moreover, the plastic analysis of an elastic - perfectly plastic solid follows from the elastic analysis quite naturally and easily. Therefore, ST. VENAN'TS theory of elastic torsion has been briefly discussed below, before considering the general method of solution of elastic - ideally plastic torsion problems.

2.1 ELASTIC TORSION

A portion of a prismatic bar, shown in Fig. (1.a), is subjected to a twisting moment T. A system of rectangular coordinates x, y, z are used, where OZ is the axis of the bar parallel to the generators and Ox and Oy lie in the plane of the cross-section. Z = O is one end of the section. Body forces due to the gravitational weight are neglected and it is further supposed

that local stress effects in the material, immediately about the point of application of T, are redistributed in a short distance to give a stress distribution across each section, which does not vary with Z.

On deforming the bar each section rotates and also warps out of its initial plane. In Fig. (1.b), P is a point whose initial coordinates are (x, y, z) and which after twisting moves from P to P' with coordinates (x + u, y + v, z + w). u, v, w are small displacements. The angle of rotation of a cross - section at a distance z from the origin is $z\theta$, where θ is the angle of twist per unit length. For elastic deformations, θ is small and is constant along the length of the bar. From Fig. (1.b) it follows that,

$$x = r\cos\beta \text{ and } y = r\sin\beta \text{ ; so that}$$
$$\delta x = -r\sin\beta\, d\beta, \quad \delta y = r\cos\beta\, d\beta,$$
$$u = \delta x = -y\delta\beta \text{ and } v = \delta y = x\delta\beta$$

Thus

$$u = -y\, z\theta \quad \text{and} \quad v = x\, z\theta \qquad (2.1.1)$$

P' is taken to have moved out of the original plane of P by an amount w. This amount varies from point to point, i.e. with x and y over the section, and can therefore be expressed as,

$$w = \theta f(x, y) \qquad (2.1.2)$$

f (x, y) is called the warping function and is assumed to be independent of z, so that warping takes place at all sections, including the ends of the bar.

From equations (2.1.1) and (2.1.2) the strain components can be expressed as

$$\epsilon x = \frac{\partial u}{\partial x} = 0 \,, \quad \epsilon y = \frac{\partial v}{\partial y} = 0 \,, \quad \epsilon z = \frac{\partial w}{\partial z} = 0$$

$$\gamma xy = \frac{\partial u}{\partial y} + \frac{\partial v}{\partial x} = -z\theta + z\theta = 0$$

$$\gamma yz = \frac{\partial v}{\partial z} + \frac{\partial w}{\partial y} = x\theta + \theta \frac{\partial f}{\partial y} \qquad (2.1.3)$$

$$\gamma xz = \frac{\partial y}{\partial z} + \frac{\partial w}{\partial x} = -y\theta + \theta \frac{\partial f}{\partial x}$$

It follows from Hooke's law and eqns. (2.1.3) that

$$\sigma x = \sigma y = \sigma z = \tau xy = 0$$

and that,

$$\tau yz = G \gamma yz = G\theta \left(x + \frac{\partial f}{\partial y} \right) \qquad (2.1.4)$$

$$\tau xz = G \gamma xz = G\theta \left(-y + \frac{\partial f}{\partial x} \right)$$

The elimination of the warping function from eqns. (2.1.4) gives,

$$\frac{\partial \tau xz}{\partial y} - \frac{\partial \tau yz}{\partial x} = -2G\theta \qquad (2.1.5)$$

With the stresses given by eqns. (2.1.4) the equations of

equilibrium for this case reduce to;

$$\frac{\partial \tau_{yz}}{\partial y} + \frac{\partial \tau_{zx}}{\partial x} = 0 \qquad (2.1.6)$$

Next, it is assumed that a function $\psi(x,y)$ exists which is capable of yielding the shear stresses and satisfying the equilibrium equation (2.1.6).

By taking

$$\tau_{xz} = \frac{\partial \psi}{\partial y} \quad \text{and} \quad \tau_{yz} = -\frac{\partial \psi}{\partial x} \qquad (2.1.7)$$

equation (2.1.6) is satisfied and equation (2.1.5) becomes

$$\frac{\partial^2 \psi}{\partial x^2} + \frac{\partial^2 \psi}{\partial y^2} = -2G\theta \qquad (2.1.8)$$

or $$\nabla^2 \psi = -2G\theta$$

ψ is called the stress function.

By differentiating equation (2.1.4) it follows that

$$\frac{\partial \tau_{xz}}{\partial x} = G\theta \frac{\partial^2 f}{\partial x^2} \quad \text{and} \quad \frac{\partial \tau_{yz}}{\partial y} = G\theta \frac{\partial^2 f}{\partial y^2}$$

On substituting these equations in eqn. (2.1.6), it follows that

$$\frac{\partial^2 f}{\partial x^2} + \frac{\partial^2 f}{\partial y^2} = \nabla^2 f = 0 \qquad (2.1.9)$$

Now, supposing that the boundary of the section is defined by points (x,y) such that $x = x(s)$ and $y = y(s)$,

where s is arc length parameter measured from some fixed point on the boundary. In Fig. (1.c) a part of the section of the bar which is perpendicular to the axis of the bar has been shown. Considering the triangular element shown at the boundary, the shear stresses over an end face of the triangular area dA, are τ_{xz} and τ_{zy}. Together, these must be such that they produce no resultant force normal to ds, because there is no normal stress over the curved surface of the bar. This gives

$$\frac{\tau_{zy}}{\tau_{zx}} = \frac{dy/ds}{dx/ds} \qquad (2.1.10)$$

Substituting from eqn. (2.1.7) in eqn. (2.1.10) it follows that

$$\frac{\partial \psi}{\partial x}\,\frac{dx}{ds} + \frac{\partial \psi}{\partial y}\,\frac{dy}{ds} = 0$$

so that $\frac{d\psi}{ds} = 0$

or $\psi =$ constant, along the boundary of the cross section. (2.1.11)

This is true for any boundary, whether it be an external one as in the case of a solid section or an internal one as for a hollow section.

The torque T, required to give a twist θ will be given by,

$$T = \int (x \tau_{zy} - y \tau_{zx}) \, dA$$

$$= -\iint \left(x \frac{\partial \psi}{\partial x} + y \frac{\partial \psi}{\partial y} \right) dx \, dy$$

using eqn. (2.1.7)

$$= \int dy \int x \frac{\partial \psi}{\partial x} \, dx - \int dx \int y \frac{\partial \psi}{\partial y} \, dy$$

If the section is not a hollow one, then integration by parts gives,

$$T = - \int dy \left[x\psi - \int \psi \, dx \right]_{x_1}^{x_2} - \int dx \left[y\psi - \int \psi dy \right]_{y_3}^{y_4}$$

(2.1.12)

where, (x_1, y_1), (x_2, y_1), (x_3, y_3), (x_3, y_4) are the points on the boundary as shown in Fig. (1.d).

Thus,

$$T = - \int dy \left[x_2\psi_2 - x_1\psi_1 - \int_{x_1}^{x_2} \psi \, dx \right]$$

$$- \int dx \left[y_4\psi_4 - y_3\psi_3 - \int_{y_3}^{y_4} \psi \, dy \right]$$

$$= 2 \iint_A \psi \, dx \, dy \qquad (2.1.13)$$

provided ψ, which is a constant along the boundary, is

taken to be zero on the boundary ($\psi_1 = \psi_2 = \psi_3 = \psi_4 = 0$). Thus for eqn. (2.1.13) to hold ψ must be taken to be zero on the boundary.

Summarizing the above results, if a function $\psi(x, y)$ can be found which is zero on the boundary of the section being twisted, and satisfies $\nabla^2\psi + 2G\Theta = 0$ then the shear stress distribution throughout the section and the torque T can be found. The magnitude of the resultant shear stress at any point will be

$$\sqrt{\left(\frac{\partial\psi}{\partial x}\right)^2 + \left(\frac{\partial\psi}{\partial y}\right)^2} = \left|\text{grad } \psi\right| \qquad (2.1.14)$$

2.2 ELASTIC - PERFECTLY PLASTIC TORSION

It was shown in the last section that $|\text{grad}\,\psi|$ represents the total shearing stress at a point. Physically, this is the maximum slope at that point of the ψ surface (as in the membrane analogy). If K denotes the yield shear stress of the bar, then for yielding at a point

$$|\text{grad}\,\psi| = K$$

Thus a limit is set on the value that the gradient at a point may attain. A further increase in the torque leads to a spread of the area over which yielding occurs. Constancy of the gradient in the membrane analogy may be simulated by erecting a constant slope roof over the section. An extension of the membrane analogy was given by Nadai[15] (1923 & '50). In this analogy it is assumed that the membrane under an increasing pressure is raised out of its plane, maintaining its largest gradient on the boundary and, having attained the critical slope, proceeds to have increasing contact with the underside of the roof.

In this manner a physical and intutive idea of the growth of the zones of plastic vielding under increasing torque may be had. From this analogy it becomes clear that in general, yielding usually proceeds from the boundary inwards towards the centroidal axis.

Throughout the outer plastic zones, the slope or yield stress is constant whereas within the section, the slope varies or the total shear stress decreases from K (assuming the material to be perfectly plastic) at the elastic - plastic boundary to zero on the axis of twist. To summarize, ψ satisfies,

$$\frac{\partial^2 \psi}{\partial x^2} + \frac{\partial^2 \psi}{\partial y^2} = -2G\theta \quad \text{in the elastic region}$$

and

$$\left(\frac{\partial \psi}{\partial x}\right)^2 + \left(\frac{\partial \psi}{\partial y}\right)^2 = K^2 \quad \text{in the plastic region}$$

and is zero on the boundary of the section.

GENERAL METHOD OF SOLUTION

For the convenience of mathematical discussion, the problem is better understood as consisting of two parts. The first part consists of obtaining a solution to the elastic problem.

Let R be a given region with Γ as its boundary as shown in Fig. (2.a). In R, it is required to solve the equation

$$\nabla^2 \psi = -2G\theta = -C \text{ (constant)} \qquad (2.2.1)$$

with $$\psi = 0 \quad \text{on the boundary } \Gamma \qquad (2.2.2)$$

Suppose that the answer to this problem has been obtained, then the quantity

$$q = \left\{ \left(\frac{\partial \psi}{\partial x}\right)^2 + \left(\frac{\partial \psi}{\partial y}\right)^2 \right\}^{\frac{1}{2}} \qquad (2.2.3)$$

can be determined. From this it is possible to find

the maximum value of q in $R + \Gamma$. Then by multiplying ψ throughout by (K/q) the elastic solution corresponding to one point just reaching the yield point can be obtained. Thus, this part of the problem corresponds to obtaining the elastic solution over the entire cross-section when yielding has just started.

The second part of the problem consists of considering the complete elastic problem (Fig. 2.b). The region R is now subdivided into two portions R_1 and R_2 (elastic and plastic), with external boundaries Γ_1 and Γ_2. The position of the common boundary D, which is the elasto-plastic boundary is not known. Now in R_1, equation

$$\frac{\partial^2 \psi_a}{\partial x^2} + \frac{\partial^2 \psi_a}{\partial y^2} = -aC, \quad a > 1 \qquad (2.2.5)$$

has to be satisfied, where a is the ratio of the new angular twist θ to θ_0, and C being the same constant as in eqn. (2.2.1).

On the boundary Γ_1 $\quad \psi_a = 0 \qquad (2.2.6)$

In R_2, which is the plastic region, stresses will throughout be K only (material considered being

ideally plastic). Hence the eqn. to be satisfied in this region is

$$\left\{\left(\frac{\partial\bar{\Psi}}{\partial x}\right)^2 + \left(\frac{\partial\bar{\Psi}}{\partial y}\right)^2\right\}^{\frac{1}{2}} = K \qquad (2.2.7)$$

On the boundary Γ_2, $\bar{\Psi} = 0$ (2.2.8)

At all points on the common boundary D, the requirement is $(\bar{\Psi})_D = (\Psi_a)_D$ (2.2.9)

But this condition is not sufficient to define the position of D uniquely; a second condition is necessary. This condition is that at any point 0 on D

$$\left(\frac{\partial\Psi_a}{\partial\underset{\sim}{l}}\right)_0 = \left(\frac{\partial\bar{\Psi}}{\partial\underset{\sim}{l}}\right)_0 \qquad (2.2.10)$$

where, $\underset{\sim}{l}$ is the common normal to the boundary. From eqns. (2.2.9) and (2.2.10) it follows that

$$\left(\frac{\partial\Psi_a}{\partial x}\right)_0 = \left(\frac{\partial\bar{\Psi}}{\partial x}\right)_0$$

and (2.2.11)

$$\left(\frac{\partial\Psi_a}{\partial y}\right)_0 = \left(\frac{\partial\bar{\Psi}}{\partial y}\right)_0$$

Now, eqn. (2.2.9) with either of the eqns. (2.2.11) is sufficient to define the position of the elasto-plastic boundary D.

The equation for the plastic region (eqn. (2.2.7)) merely states the fact that in R_2 (plastic region) the maximum slope of $\bar{\psi}$ is everywhere constant and has the value K.

By virtue of equation (2.2.8) the contours of constant $\bar{\psi}$ will, therefore, be lines parallel to the boundary Γ_2. Thus equation (2.2.7) can easily be satisfied for any region R_2 and, infact, the solution is independent of the position of D. The portion R_2 has been shown separately in Fig. (2.C) with its boundary Γ_2. Contours of constant $\bar{\psi}$, namely C_1, C_2 and C_3 are shown at equal intervals d, which are all drawn parallel to Γ_2. On C_1, $\bar{\psi}$ will have the value

$$(\bar{\psi})_{C_1} = \frac{\partial \bar{\psi}}{\partial N} d \qquad \text{since } (\bar{\psi})_{\Gamma_2} = 0$$

$$= Kd \qquad (2.2.12)$$

N being the measured normal to the boundary.

The value of $\bar{\psi}$ on the other contours can be evaluated in a similar manner. In this way, working inwards from the boundary a solution of equation (2.2.7) for $\bar{\psi}$ can be built up which will hold everywhere inside region R_2, irrespective of what happens in R_1, and also

irrespective of the actual position of the boundary D. The solution depends on the shape of the boundary Γ_2 and on the value of K, which is the yield stress in pure torsion. The real problem, ofcourse, is to find the elastic plastic boundary where the matching conditions given by eqns. (2.2.9) and (2.2.10) are to be satisfied.

By adopting a iterative technique the second part of the problem can be solved completely, once the first part of the problem has already been solved. The entire discussion is based on a finite difference representation which can be summarized as follows:

(i) using the method which has just been described, a solution $\bar{\psi}$ is constructed at the different mesh points. The two curves, shown in Fig.(3.a), represent the traces of the function $\bar{\psi}(x,y)$, $\psi(x,y)$ on a plane perpendicular to the x,y plane. A is supposed to be the point on the boundary where the maximum value of q, i.e K occurs; and N is the normal to the boundary. The very method of constructing $\bar{\psi}$ makes the two curves tangential at A.

(ii) Multiplying the elastic solution ψ of the first part of the problem by a known number $a = \theta/\theta_0$,

the first approximation to ψ_a is obtained as $\psi_a = a\psi$. This solution will have values greater than those of $\bar{\psi}$ at some points; and the line of intersection of the two surfaces $\bar{\psi}$ and ψ_a can be determined by interpolation. This line has been indicated by point (1) in Fig.(3.b). However, the condition that the two surfaces be tangential at the boundary is not satisfied.

(iii) The position of the common boundary D is adjusted by keeping it on the $\bar{\psi}$ surface and at the same time by keeping all the values of ψ_a fixed, except those on the common boundary, until the tangential matching condition (2.2.11) is approximately satisfied. This can be done by using the finite difference formula for first derivatives. In this way the boundary D shifts to a new position, as is shown in Fig. (3.b) by point (2).

(iv) Now, since the position of D and the value of ψ_a on D have both been modified, eqn. (2.2.5) is no longer satisfied at points such as (3) (shown in Fig. (3.b)). Keeping the new boundary values and the boundaries fixed, the solution to eqn. (2.2.5) is obtained in R_2 by relaxation or

anyother method. This, however, gives rise to a violation of the "tangent" condition. But, for this new solution the lack of agreement in the tangent condition will not be as bad as that in (ii) if the initial guess is good.

(v) In this way the position of the common boundary is readjusted as explained in (iii) and the complete procedure, described above, is repeated until both equations (2.2.5) and (2.2.11) are satisfied simultaneously.

In this way a desired solution is obtained, since the requirements of equations (2.2.7), (2.2.8) and (2.2.9) are automatically satisfied. After a few iterations of the above procedure a complete solution of the problem is obtained.

The solution of elastic - ideally plastic torsion has been thoroughly investigated by many authors for different shapes of the cross-section. The references for this have already been given in the section 1. The detailed procedure which has been described above is due to F.S. Shaw[16]. He used the relaxation technique based on finite differences.

3. FORMULATION OF THE TORSION PROBLEM FOR WORK HARDENING MATERIALS

The elastic - ideally plastic model is a highly idealized model. In fact, there is always some work hardening associated with deformations beyond the elastic limit. Therefore, to obtain information about stress concentration and the plastic zone, particularly for the materials whose nature of deformation in the plastic range is far from being ideally plastic, strain hardening effects have to be taken into account. The primary purpose of this section is to consider the differential equation of plastic torsion. However, since the coefficients in this equation are a function of the inelastic properties of the material, a brief discussion of the assumed yield criterion and non - linear stress - strain relations, as well as some comments on the deformation theory and strain hardening have been given, before deriving the differential equation governing plastic torsion.

3.1 CRITERION FOR YIELDING

A law defining the limit of elasticity under any possible combination of stresses is known as criterion for yielding or yield criterion. The two simplest and most widely used yield criteria, which are consistent with experimental evidence, are the criterion of TRESCA and the criterion due

to VON MISES'. For most metals, Von Mises' law fits the experimental results more closely than Tresca's, but Tresca's criterion is simpler to use in theoretical applications. In this thesis the Von Mises yield criterion has been utilized. For a general state of stress, in terms of the cartesian coordinates, this criterion postulates that yielding occurs, when

$$J_2 = \frac{1}{6}\left[(\sigma_x - \sigma_y)^2 + (\sigma_y - \sigma_z)^2 + (\sigma_z - \sigma_x)^2 + 6(\tau_{xy}^2 + \tau_{xz}^2 + \tau_{yz}^2) \right] = K^2$$

where, K is a parameter dependent on the amount of pre-strain.

As explained by Hill[17], certain assumptions and simplifications which are consistent with experimental evidence are made in arriving at a criterion of yielding. For the purpose of this thesis, the following assumptions are pertinent.

(i) Time - dependent effects are not considered; this means, for example, that creep and thermal and viscous effects are dis-regarded.

(ii) The Bauschinger effect is also disregarded since only a monotomically increasing torque has been considered.

(iii) The material is assumed to be isotropic throughout its strain history, since large inelastic deformations are precluded.

(iv) A hydrostatic state of stress has no effect on the yielding of the material.

3.2 STRAIN HARDENING

The concept of strain-hardening or work hardening in simple tension implies that the strain is a monotomically increasing function of the stress. This means that the stress necessary for continued plastic deformation increases with the increase of plastic deformation. This coincides with the definition of a stable elastic - plastic material, which requires positive work to be done during any cycle of loading. If beyond some point the material exhibits a falling stress - strain curve then this portion would be classified as unstable.

A widely accepted general definition of strain - hardening has been given by Drucker[18]. Suppose a body is in equilibrium and subjected to surface fraction F_i and body forces B_i. Now, by means of δF_i and δB_i, the stresses are first slowly increased and then slowly decreased by removing

δF_i and δB_i. Strain-hardening implies that for all such added sets of stresses the material will remain in equilibrium and that

(a) Positive work is done by δF_i and δB_i during the application of the added set of stresses.

(b) The net work done due to δF_i, δB_i during a cycle of application and removal is positive if plastic deformation has occured in the cycle, or zero if only elastic changes of strains are produced. This definition of strain hardening is widely accepted since it is in agreement with experimental studies.

Assuming that a strain hardening material obeys the Von Mises yield criterion and Y_0 is the initial yield stress, then the radius of the Mises circle, or yield locus, is $\frac{\sqrt{2}}{3} Y_0$. Further plastic straining alters the current yield locus. If the straining is continued to Y_1 and the strains are then completely removed and if isotropy is assumed throughout the cycle, the material now possesses a yield locus which is a circle of radius $\frac{\sqrt{2}}{3} Y_1$. The latter circle will be concentric with the former circle. Such a material is called an isotropic strain - hardening material. The yield locus retains its shape but expands with the stress and

strain history. This concept of isotropic strain - hardening facilitates the mathematics of the problem, but may in reality be considered only as a first approximation.

3.3 DEFORMATION THEORY

The deformation theory of plasticity is due to Hencky and Nadai. The term deformation theory was given by Il'iwshin. This theory assumes that, as in the theory of elasticity, there exists a one to one correspondence between the stress and strain.

The popularity of the deformation theory may be attributed to its mathematical simplicity as well as due to its agreement with early experiments in which the stress ratios remained constant. Flow and deformation theories themselves agree if the stress ratios remain constant. It is well known that the deformation theory is inadequate in cases wherein there are large departures from proportionality. However, when this does not occur, this theory can be considered to be less objectionable. Based on Drucker's[18] thermodynamic definition of work hardening it has been proved by Budianskey[11] (1959), that the deformation theory is consistent with the flow theory for some restricted paths of loading apart from proportional loading.

A general stress strain relation, based on the deformation theory, which was proposed by W. Prager[19] (1945) is given by

$$\underset{\sim}{\varepsilon} = f\,(J_2, J_3^2)\,\Big[\,p\,(J_2, J_3^2)\,J_3\,\underset{\sim}{T} + q\,(J_2, J_3^2)\,\underset{\sim}{S} \tag{3.3.1}$$

where, $$\underset{\sim}{T} = \underset{\sim}{S}^2 - 2/3\,J_2\,\underset{\sim}{I} \tag{3.3.2}$$

and p, q are polynomials, which are homogeneous in the stress components.

Prager, has also discussed some special cases of the general relation given by eqn. (3.3.1). One of the simplest relations is obtained by putting $p = 0$, $q = 1$ and by assuming f to be a function of J_2 only. The resulting relation is of the form,

$$\underset{\sim}{\varepsilon} = f\,(J_2)\,\underset{\sim}{S} \tag{3.3.3}$$

This particular stress strain relation stipulates that the ratios of the principal strains equals the ratios of the principal components of the stress deviator.

3.4 NON-LINEAR ELASTIC PLASTIC BEHAVIOUR

The non-linear elastic plastic behaviour, which has been considered here, is of the type discussed by Ramberg and

Osgood[14] (1943) for explaining the tensile stress-strain relations for certain materials. Ramberg and Osgood have shown that most of the stress strain curves in tension can be represented by the relation

$$\epsilon = \frac{\sigma}{E}\left[1 + \alpha\left(\frac{\sigma}{\sigma_o}\right)^{n-1}\right] \qquad (3.4.1)$$

If all the stress components are non-dimensionalized by the yield stress σ_Y and the strainsare normalized with respect to the corresponding yield strain, $\epsilon_Y = \frac{\sigma_Y}{E}$, then eqn. (3.4.1) reduces to

$$\bar{\epsilon} = \bar{\sigma} + \alpha\bar{\sigma}^{n} \qquad (3.4.2)$$

where, $\alpha = 0.02$ (approx.), corresponding to the usual engineering definition of yield.

Tensile curves for $\alpha = 0.02$ have been shown in Fig. (7), for several values of the strain hardening coefficient n.

The application of eqn. (3.4.2) is restricted to monotomically increasing stress or more commonly to conditions of no unloading.

In this thesis, only the simplest deformation theory has been employed. Plastic deformation is assumed to be

independent of the hydrostatic component of stress $\frac{1}{3}\,\bar{\sigma}_{kk}$, and is also assumed to be completely determined by the second invariant of the stress deviator

$$S_{ij} = \bar{\sigma}_{ij} - \frac{1}{3}\,\bar{\sigma}_{kk}\,\delta_{ij} \qquad (3.4.3)$$

(The first invariant being identically zero)

The invariant has been introduced in the form of the "effective stress" $\bar{\sigma}_e$ defined by

$$\bar{\sigma}_e^{\,2} = \frac{3}{2}\,\bar{S}_{ij}\,\bar{S}_{ij} \qquad (3.4.4)$$

Thus in simple tension $\bar{\sigma}_e = \bar{\sigma}$; and the Mise's yield criterion, for this theory, reduces to $\bar{\sigma}_e = 1$. Ofcourse, a smooth representation such as given by eqn. (3.4.2) admits only an effective or approximate yield condition.

Now, a generalized stress-strain relation which reduces to eqn. (3.4.2) in simple tension is

$$\bar{\epsilon}_{ij} = (1+\nu)\,\bar{S}_{ij} + \left(\frac{1-2\nu}{3}\right)\bar{\sigma}_{pp}\,\delta_{ij} + \frac{3}{2}\alpha\left(\frac{n-1}{\bar{\sigma}_e}\right)\bar{S}_{ij} \qquad (3.4.5)$$

This is the final form of the stress-strain relation which has been made use of in deriving the equations of plastic torsion. This type of a relation has recently been used by many authors.[20]

PIECEWISE LINEAR RELATION

A somewhat less realistic representation of the tensile stress - strain behaviour of common metals, other than the Ramberg - Osgood relation, is the piecewise linear relation. However, this approximation does model certain features of plastic flow. In particular, the behaviour of Alluminium alloys is very closely approximated by this type of an idealization. The assumption of piecewise linearity states that in each plastic regime (i.e side or corner), there exists a relationship, between the stress rates and the strain rates, whose coefficients are material constants which are independent of the strain history of the material. In addition, the effect of strain hardening upon the behaviour of the yield condition itself is also linear.

For such an idealization, the general stress - strain relation is given by

$$\bar{\epsilon}_{ij} = (1+\nu)\,\bar{\sigma}_{ij} - \nu\,\bar{\sigma}_{pp}\,\delta_{ij} + \lambda(1-\bar{\sigma}_e^{-1})\,\bar{S}_{ij}$$

where $\lambda = \frac{3}{2}\left(\frac{E}{E_t} - 1\right)$ if $\bar{\sigma}_e > 1$

and $\lambda = 0$ if $\bar{\sigma}_e \leq 1$

Using this relation, the equations of plastic torsion have been derived for the piecewise linear behaviour of materials also.

3.5 PLASTIC - TORSION

In deriving the equation for the plastic torsion it has been assumed that the basic assumptions of the theory of elastic torsion are still valid for the elastic - plastic state, except that a different stress - strain relation has been employed. That is to say that, even on the portions of the cross section which have become plastic the only non-zero components of the stress and strain are

$$\tau_{xz} \text{ , } \tau_{yz} \text{ and } \gamma_{xz} \text{ , } \gamma_{yz} \text{ .}$$

Further, in order to keep the mathematics of the stress - strain relations as simple as possible without losing the essential features of the theory, the plastic meterial has been considered to be incompressible. All viscosity effects have been neglected, that is, the stress-strain relation has been assumed to be independent of the speed of deformation. For moderate strain rates and temperatures both the assumptions are well justified for structural metals.

Now, starting with equation (2.1.3), it is clear that

$$\epsilon_x = \epsilon_y = \epsilon_z = \epsilon_{xz} = 0 \qquad (3.5.1)$$

and

$$\gamma_{xz} = \frac{\partial w}{\partial x} - \theta y$$
$$\gamma_{yz} = \frac{\partial w}{\partial y} + \theta x \qquad (3.5.2)$$

Because only two components of the stress, namely τ_{xz} and τ_{yz} have been assumed to be non - zero, the first invariant of stress,

$$I = \sigma_{kk} = 0 \qquad (3.5.3)$$

Substituting zero for $_{kk}$ in eqn. (3.4.3) and (3.4.5) gives

$$S_{ij} = \sigma_{ij} \qquad (3.5.4)$$

and

$$\bar{\epsilon}_{ij} = (1+\nu)\,\bar{S}_{ij} + \frac{3}{2}\alpha\,\bar{\sigma}_e^{\,n-1}\,\bar{S}_{ij} \qquad (3.5.5)$$

Replacing S_{ij} by σ_{ij} from eqn. (3.5.4), and expanding equation (3.4.4), the value of the effective stress comes out to be

$$\bar{\sigma}_e = \sqrt{3}\left[\tau_{xz}^2 + \tau_{yz}^2\right]^{\frac{1}{2}} \qquad (3.5.6)$$

Once again, assuming that a stress function ψ exists such that

$$\bar{\tau}_{xz} = \frac{\psi_y}{\sigma_Y} \quad , \quad \bar{\tau}_{yz} = -\frac{\psi_x}{\sigma_Y} \tag{3.5.7}$$

the expression for $\bar{\sigma}_e$ reduces to

$$\bar{\sigma}_e = \frac{\sqrt{3}}{\sigma_Y}\left[\psi_x^2 + \psi_y^2\right]^{\frac{1}{2}} \tag{3.5.8}$$

The generalized stress - strain relation given by eqn. (3.4.5) gives

$$\bar{\epsilon}_{xz} = (1+\nu)\,\bar{\tau}_{xz} + \frac{3}{2}\alpha\,\bar{\sigma}_e^{n-1}\,\bar{\tau}_{xz}$$

and

$$\bar{\epsilon}_{yz} = (1+\nu)\,\bar{\tau}_{yz} + \frac{3}{2}\alpha\,\bar{\sigma}_e^{n-1}\,\bar{\tau}_{yz} \tag{3.5.9}$$

which on substituting the values of the stress components $\bar{\tau}_{xz}$ and $\bar{\tau}_{yz}$ from eqn. (3.5.7), reduces to

$$\bar{\epsilon}_{xz} = \left\{(1+\nu) + \frac{3}{2}\alpha\,\bar{\sigma}_e^{n-1}\right\}\psi_y / \sigma_Y$$

and

$$\bar{\epsilon}_{yz} = -\left\{(1+\nu) + \frac{3}{2}\alpha\,\bar{\sigma}_e^{n-1}\right\}\psi_x / \sigma_Y \tag{3.5.10}$$

Next, by expressing the strain components in terms of the displacements and its derivatives from eqn. (3.5.2), eqns. (3.5.10) gives

$$\frac{1}{2}\left(\frac{\partial w}{\partial x} - \theta y\right) E = \left\{(1+\nu) + \frac{3}{2}\alpha\,\bar{\sigma}_e^{\,n-1}\right\}\psi_y \qquad (3.5.11)$$

and

$$\frac{1}{2}\left(\frac{\partial w}{\partial y} + \theta x\right) E = -\left\{(1+\nu) + \frac{3}{2}\alpha\,\bar{\sigma}_e^{\,n-1}\right\}\psi_x \qquad (3.5.12)$$

Differentiating eqn. (3.5.11) with respect to y and eqn. (3.5.12) with respect to x and subtracting, we get

$$-\theta E = \left\{(1+\nu) + \frac{3}{2}\alpha\,\bar{\sigma}_e^{\,n-1}\right\}\nabla^2\psi + \frac{3}{2}\alpha(n-1)\,\bar{\sigma}_e^{\,n-2}\left\{(\bar{\sigma}_e)_y\,\psi_y + (\bar{\sigma}_e)_x\,\psi_x\right\} \qquad (3.5.13)$$

Or

$$\begin{aligned} -\theta E &= \left\{(1+\nu) + \frac{3}{2}\alpha\,\bar{\sigma}_e^{\,n-1}\right\}\nabla^2\psi + \frac{3}{2}\alpha(n-1)\,\bar{\sigma}_e^{\,n-2} \\ &\quad \left\{(\bar{\sigma}_e\psi_x)_x + (\bar{\sigma}_e\psi_y)_y - \bar{\sigma}_e\,\nabla^2\psi\right\} \\ &= \left\{(1+\nu) + \frac{3}{2}\alpha(2-n)\,\bar{\sigma}_e^{\,n-1}\right\}\nabla^2\psi + \\ &\quad \frac{3}{2}\alpha(n-1)\,\bar{\sigma}_e^{\,n-2}\left\{(\bar{\sigma}_e\psi_x)_x + (\bar{\sigma}_e\psi_y)_y\right\} \end{aligned} \qquad (3.5.14)$$

This is the final form of the differential equation which is supposed to govern torsion in the plastic region. It has been put in this form, instead of writing $\bar{\sigma}_e$ in terms of stress function ψ and expanding all the

terms, to suit a special purpose which will be clear while discussing the numerical solution of this equation.

Similarly, for a piecewise linear stress-strain relation a separate plastic torsion equation can be derived and it comes out to be,

$$-\Theta E = \left\{(1+\nu+\lambda) - \frac{2\lambda}{\bar{\sigma}_e}\right\}\nabla^2\psi + \frac{\lambda}{\bar{\sigma}_e^2}\left\{(\bar{\sigma}_e \psi_x)_x + (\bar{\sigma}_e \psi_y)_y\right\} \qquad (3.5.15)$$

where,

$$\lambda = \frac{3}{2}\left[\frac{E}{E'} - 1\right] \quad \text{if } \bar{\sigma}_e > 1$$

$$= 0 \quad \text{if } \bar{\sigma}_e \leq 1$$

and

$$\bar{\sigma}_e = \frac{\sqrt{3}}{\sigma_Y}\left[\psi_x^2 + \psi_y^2\right]$$

3.6 NON-DIMENSIONALIZATION OF THE LENGTH SCALE

The coordinates will be non-dimensionalized as,

$$\xi = \frac{x}{L} \quad , \quad \eta = \frac{y}{L} \qquad (3.6.1)$$

where, L is a characterstic length of the prismatic bar. Further a new stress function Φ defined by

$$\Phi(\xi, \eta) = \frac{1}{L^2}\psi(x, y) \qquad (3.6.2)$$

will be used.

Substituting for the variables in terms of the non-dimensional coordinates and Φ, eqns. (2.1.8) and (3.5.4) for elastic and plastic torsion respectively reduce to,

$$\nabla^2\Phi = -2G\Theta \qquad \text{(Elastic)} \qquad (3.6.3)$$

and

$$-\Theta E = \left\{(1+\nu) + \frac{3}{2}(2-n)\alpha\,\bar{\sigma}_e^{n-1}\right\}\nabla^2\Phi + \frac{3}{2}\alpha(n-1)\,\bar{\sigma}_e^{n-2}\left\{(\bar{\sigma}_e\Phi_\xi)_\xi + (\bar{\sigma}_e\Phi_\eta)_\eta\right\} \qquad (3.6.4)$$

The stress components are given by

$$\tau_{xz} = L\Phi_\eta \quad , \quad \tau_{yz} = -L\Phi_\xi \qquad (3.6.5)$$

and therefore

$$\bar{\sigma}_e = \frac{\sqrt{3}\,L}{\sigma_Y}\left[(\Phi_\xi)^2 + (\Phi_\eta)^2\right]^{\frac{1}{2}} \qquad (3.6.6)$$

Equation (2.1.13), which gives the value of the torque, becomes

$$T = 2L^4 \iint_A \Phi\, d\xi\, d\eta \qquad (3.6.7)$$

Only these equations have been used in the solution of the problems and in the computation of the various quantities, such as the equivalent stress, torque etc.

4. METHOD OF NUMERICAL SOLUTION

There are many numerical methods for solving partial differential equations. Of all these, the method of finite-differences is used most widely because of the ease and universality of its application. This technique has proved its worth in practically every branch of science and technology; and the method has already been used by many authors for the solution of elasto-plastic problems, including that of elasto-plastic torsion. In this section of the thesis the method of finite differences has been briefly outlined and the finite difference equations for the differential equations (3.6.3) and (3.6.4) have been derived. Finally, the scheme for obtaining the elasto-plastic solution of our problem (torsion), has been discussed in detail.

4.1 METHOD OF FINITE - DIFFERENCES

The essential principle of the finite-difference technique is to replace the differentials of a variable by the differences taken over finite intervals. The field of interest is, therefore, replaced by a net of grid lines. The points of intersection of the grid are termed the "nodes" and it is with these nodes as the focii that the differential equation is integrated. The finite difference technique, therefore, represents the replacement of the

differential equations by a system of difference equations which are essentially a set of simultaneous algebraic equations involving the unknown variable at the nodes only. The solution of these simultaneous equations gives the numerical values of the unknown at these nodal points. The selection of the method for the solution of these equations depends on the order and the nature of the coefficient matrix of these equations.

For writing the difference equation three types of difference operators are used; the backward difference, the forward difference and the central difference operators. The central difference operator, being superior to the other two, has been used here; its order of convergence being h^2, (h being the grid spacing). The accuracy can be improved by using higher order finite differences but this requires the consideration of fictitious points beyond the boundary, for almost the same rate of convergence.

The specific finite difference scheme for solving equations (3.6.3) and (3.6.4) has been described below.

4.2 FINITE DIFFERENCE EQUATIONS

ELASTIC TORSION EQUATION: Equation (3.6.3) which governs elastic torsion, is Poisson's equation and has been solved by many authors, by using the finite difference technique.

The right hand side of eqn. (3.6.3) being a constant $2G\Theta$, for a given angle of twist, we need only write $\nabla^2\Phi$ in terms of finite differences. Salvadori[21] has given the finite difference operator for ∇^2 (Laplacian operator) in rectangular, polar, triangular and screw coordinates. We consider here only a rectangular grid system as shown below.

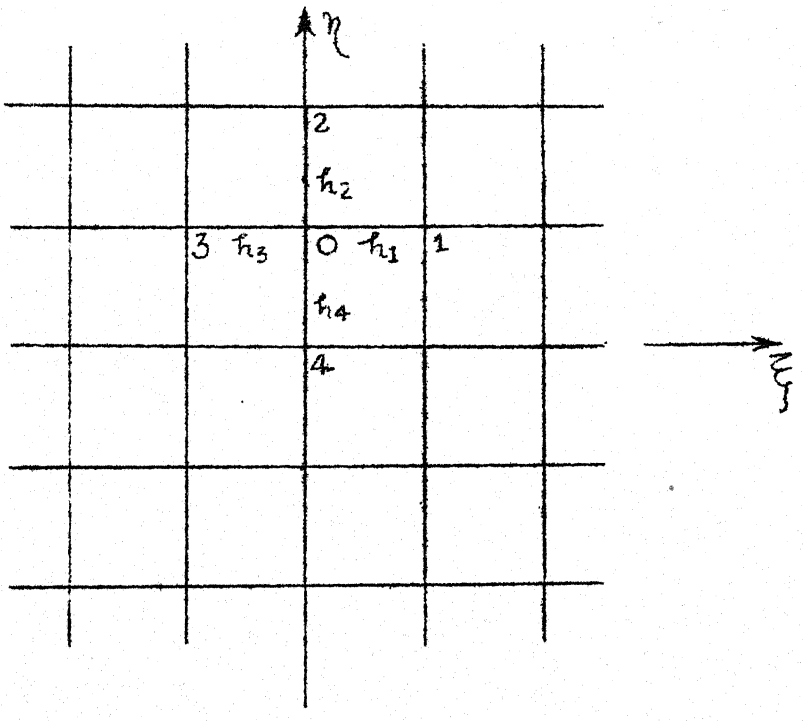

Let, 0 be one of the typical nodes at which the differential equation has to be satisfied; and let, 1, 2, 3 and 4 be the neighbouring nodes around 0. Then we know that (see Ref. 22).

$$\nabla^2 \Phi_o = -2\left[\frac{1}{h_1 h_3} + \frac{1}{h_2 h_4}\right]\Phi_o + \frac{2}{h_1+h_3}\left[\frac{\Phi_1}{h_1} + \frac{\Phi_3}{h_3}\right] + \frac{2}{h_2+h_4}\left[\frac{\Phi_2}{h_2} + \frac{\Phi_4}{h_4}\right] + \text{Error term } 0\ (h^2) \qquad (4.2.1)$$

where, h_1, h_2, h_3 and h_4 are the distances of the neighbouring nodes 1, 2, 3 and 4 respectively.

Using this difference operator given by eqn. (4.2.1) for ∇^2 and neglecting the second order error term $0\ (h^2)$, equation (3.6.3) can be replaced at the pivotal point 0, by the difference equation,

$$-2\left[\frac{1}{h_1 h_3} + \frac{1}{h_2 h_4}\right]\Phi_o + \frac{2}{h_1+h_3}\left[\frac{\Phi_1}{h_1} + \frac{\Phi_3}{h_3}\right] + \frac{2}{h_2+h_4}\left[\frac{\Phi_2}{h_2} + \frac{\Phi_4}{h_4}\right] = -2G\Theta \qquad (4.2.2)$$

If the neighbouring points are at equal distances from the point 0, say h, the equation (4.2.2) further reduces to

$$4\Phi_o - \Phi_1 - \Phi_2 - \Phi_3 - \Phi_4 = 2G\Theta h^2 \qquad (4.2.3)$$

Hence, the differential equation (3.6.3) has been transformed into a difference equation (4.2.3). Finite difference operators for ∇^2 can be chosen in other coordinate systems also and a difference equation similar to

(4.2.3) can be derived.

PLASTIC-TORSION EQUATION: The core of our computational procedure is the derivation of the finite-difference equation for the plastic-torsion equation (3.6.4). To facilitate the derivation, the L.H.S. of the equation has been considered in two parts. The first part is

$$\left\{(1+\nu) + \frac{3}{2}\alpha\,(2-n)\,\bar{\sigma}_e^{\,n-1}\right\}\nabla^2\Phi \quad \text{denoted by (I)}$$

the second part being

$$\frac{3}{2}\alpha(n-1)\,\bar{\sigma}_e^{\,n-2}\left\{(\bar{\sigma}_e\Phi_\xi)_\xi + (\bar{\sigma}_e\Phi_\eta)_\eta\right\}$$

denoted by (II)

Thus, the complete equation (3.6.4) may be written symbolically as

$$(I) + (II) = -\Theta E \quad .$$

Also, for convenience, $\bar{\sigma}_e$ has been denoted by χ. Thus,

$$(I) = \left\{(1+\nu) + \frac{3}{2}\alpha(2-n)\,\chi^{n-1}\right\}\nabla^2\Phi \qquad (4.2.4)$$

and

$$(II) = \frac{3}{2}\alpha(n-1)\,\chi^{n-2}\left\{(\chi\Phi_\xi)_\xi + (\chi\Phi_\eta)_\eta\right\} \qquad (4.2.5)$$

Once again a rectangular mesh has been chosen (as shown on page 41) and the difference equation at the node point 0 has been obtained. Finite difference equations have been derived separately for equations (4.2.4) and (4.2.5) which, when added together give the final difference equation for the differential equation (3.6.4). Considering equation (4.2.5), the difference equation for this can be written with the help of equation (4.2.2), as

$$(I) = \left\{ (1+\nu) + \frac{3}{2}\alpha(2-n)\chi_o^{n-1} \right\} \left[-2\left\{ \frac{1}{h_1 h_3} + \frac{1}{h_2 h_4} \right\} \Phi_o + \frac{2}{h_1+h_3}\left\{ \frac{\Phi_1}{h_1} + \frac{\Phi_3}{h_3} \right\} + \frac{2}{h_2+h_4}\left\{ \frac{\Phi_2}{h_2} + \frac{\Phi_4}{h_4} \right\} \right] \quad (4.2.6)$$

where,

$$\chi_o = \sqrt{3}\sqrt{\left(\frac{\partial\Phi}{\partial\xi}\right)_o^2 + \left(\frac{\partial\Phi}{\partial\eta}\right)_o^2} \Big/ \sigma_Y \quad (4.2.7)$$

Next, equation (4.2.5) is first re-written in the form

$$(II) = \frac{3}{2}\alpha(n-1)\chi^{n-2}\left\{ \frac{1}{2}\nabla^2(\chi\Phi) + \frac{1}{2}\chi\nabla^2\Phi - \frac{1}{2}\Phi\nabla^2\chi \right\} \quad (4.2.8)$$

Using the finite difference operator for ∇^2, this equation reduces to

$$(II) = \frac{3}{2}\alpha(n-1)\chi_o^{n-2}\left[\frac{\chi_1+\chi_o}{h_1(h_1+h_3)}\Phi_1 + \frac{\chi_2+\chi_o}{h_2(h_2+h_4)}\Phi_2 + \frac{\chi_3+\chi_o}{h_3(h_3+h_1)}\Phi_3 + \frac{\chi_4+\chi_o}{h_4(h_4+h_2)}\Phi_4 - \left\{\chi_o\left(\frac{1}{h_1 h_3}+\frac{1}{h_2 h_4}\right) + \frac{\chi_1}{h_1(h_1+h_3)} + \frac{\chi_2}{h_2(h_2+h_4)} + \frac{\chi_3}{h_3(h_3+h_1)} + \frac{\chi_4}{h_4(h_4+h_2)}\right\}\Phi_o\right] \quad (4.2.9)$$

where, χ_i (at the node point i) can be calculated from equation (4.2.7). It must be borne in mind that χ_i can never be negative. Combining equations (4.2.6), (4.2.7) and (4.2.9), the complete finite difference scheme for equation (3.6.4) comes out to be,

$$\left\{(1+\nu)+\frac{3}{2}\alpha(2-n)\,\chi_o^{\,n-1}\right\}\left[-2\left\{\frac{1}{h_1 h_3}+\frac{1}{h_2 h_4}\right\}\Phi_o\right.$$

$$\left.+\frac{2}{h_1+h_3}\left\{\frac{\Phi_1}{h_1}+\frac{\Phi_3}{h_3}\right\}+\frac{2}{h_2+h_4}\left\{\frac{\Phi_2}{h_2}+\frac{\Phi_4}{h_4}\right\}\right]$$

$$+\frac{3}{2}\alpha(n-1)\,\chi_o^{\,n-2}\left[\frac{\chi_1+\chi_o}{h_1(h_1+h_3)}\Phi_1+\frac{\chi_2+\chi_o}{h_2(h_2+h_4)}\Phi_2\right.$$

$$\left.+\frac{\chi_3+\chi_o}{h_3(h_3+h_1)}\Phi_3+\frac{\chi_4+\chi_o}{h_4(h_4+h_2)}\Phi_4\right.$$

$$-\left\{\chi_o\left(\frac{1}{h_1 h_3}+\frac{1}{h_2 h_4}\right)+\frac{\chi_1}{h_1(h_1+h_3)}+\frac{\chi_2}{h_2(h_2+h_4)}\right.$$

$$\left.\left.+\frac{\chi_3}{h_3(h_3+h_1)}+\frac{\chi_4}{h_4(h_4+h_2)}\right\}\Phi_o\right]=-\Theta E \qquad (4.2.10)$$

If, the mexh is assumed to be square, such that $h_1 = h_2 = h_3 = h_4 = h$ (say) then, equation (4.2.10) further reduces to

$$\left\{(1+\nu)+\frac{3}{2}\alpha(2-n)\,\chi_o^{\,n-1}\left[-4\Phi_o+\Phi_1+\Phi_2+\Phi_3+\Phi_4\right]\right.$$

$$+\frac{3}{2}\alpha(n-1)\,\chi_o^{\,n-2}\left[\frac{\chi_1+\chi_o}{2}\Phi_1+\frac{\chi_2+\chi_o}{2}\Phi_2\right.$$

$$\left.+\frac{\chi_3+\chi_o}{2}\Phi_3+\frac{\chi_4+\chi_o}{2}\Phi_4-\sum_{i=1}^{4}\frac{\chi_i+\chi_o}{2}\Phi_o\right.$$

$$=-\Theta E.h^2 \qquad (4.2.11)$$

Since, this finite difference equation is based on the values of $\overline{\sigma_e}$ (or χ) at the nodal points which have first to be calculated by finding out the derivatives of the stress function Φ , it is obvious that the solution can be obtained by an iterative process only. To start the solution a current set of values for Φ will have to be generated.

4.3 ELASTO-PLASTIC SOLUTION

After developing the finite difference equations, both for the elastic and the plastic torsion, a procedure for obtaining the elasto-plastic solution will be laid down. First we consider the criterion that has to be satisfied to obtain the required solution. Naturally, the elastic and plastic equations (3.6.3) and (3.6.4) should be satisfied in their respective domains. At the boundary the stress function surface should be smooth so that the resultant shear stress is continuous at the elasto-plastic boundary. The computational procedure which has been used to obtain the solution can be summarised as follows:

(i) The region under consideration is covered by a rectangular grid. It is assumed that the Φ surface passing over the nodal points

has nearly the same properties as the actual stress surface, that is, its contours and gradients will give the direction and the magnitude of the shear stresses respectively.

(ii) The elastic torsion equation is first solved over the entire section. To achieve this the difference equation is written corresponding to every node by using eqn. (4.2.2). In this way a set of algabraic simultaneous equations are obtained, which can be solved to give the values of Φ at the pivotal points. Since the number of simultaneous equations is generally more than a hundred, an iterative method has to be used for their solution. In this thesis, the Gauss-Seidel iteration method has been used, the details of which are given in appendix (A).

With the help of these values of Φ at the nodes, Φ_ξ , Φ_η and hence the resultant shear stress $\overline{\sigma_e}$ can be calculated by using eqn. (4.2.7).

(iii) As a first approximation, we can assume that the nodes at which the values of the non-dimensional stress $\bar{\sigma}_e$ (or χ), exceeds one become plastic. Corresponding to such nodes the finite difference equation is re-written using eqn. (4.2.10) and the previously calculated values of $\bar{\sigma}_e$. The difference equation corresponding to the other nodes remains unchanged since they still lie in the elastic region.

(iv) This new set of simultaneous equations is solved for Φ. After this, the values of Φ_ξ, Φ_η and hence of $\bar{\sigma}_e$ (or χ) are calculated at every node again.

(v) By using these values of $\bar{\sigma}_e$ the nodes are tested for being elastic or plastic by finding as to whether the values of $\bar{\sigma}_e$ are smaller or greater than one.

Some new nodes may enter into the plastic region, whereas some of the nodes which were in the plastic region may become elastic.

Therefore, the coefficient matrix of the simultaneous equations is again modified by re-writing the difference equations for all the nodes lying in the plastic zone by using equation (4.2.10). For the nodes which have become elastic (from plastic), the difference equation is re-written by applying the difference equation (4.2.2).

(vi) Steps (iv) and (v) are then repeated till the values of Φ converge giving a stable stress distribution. In fact, the values of Φ and $\overline{\sigma_e}$ and hence of the elasto - plastic boundary will keep changing after every iteration.

Depending on the number of iterations and ofcourse on the mesh size any reasonable degree of accuracy can be achieved.

(vii) Lastly, when the values of Φ and $\overline{\sigma_e}$ have converged, the elasto-plastic boundary can be found by interpolation by using the criterion that the value of $\overline{\sigma_e}$ has to be one on it. Either a linear or a higher order interpolation formula can be used.

In going through the above steps (from (i) to (vii), the elastic and the plastic equations (3.6.3) and (3.6.4) have been satisfied in their respective regions. With regard to the smoothness of the stress function ϕ and the shear stress χ, the method of finite differences itself implies that the derivative is continuous. No attempt has been made to justify this here.

5. RESULTS AND DISCUSSION

5.1 APPROPRIATE MESH SIZE

Since the numerical technique described in the previous section is based on finite difference approximations, it becomes necessary to decide an appropriate mesh size which will give a solution converging to the actual one. By carrying out the actual computation, it was found that the size of the suitable mesh depends on the shape of the cross-section. If in a direction, the gradient of the stress function (resultant shear stress) is expected to change rapidly, then a finer mesh must be used in that direction. This is necessary because the coefficients of the matrix in a row, corresponding to a node lying in the plastic region, are effected by the values of $\bar{\sigma}_e$ at its neighbouring nodes raised to the (n-1) power. Therefore, if the nodes are not sufficiently close, the diagonal nature of the matrix is not preserved and this leads to overflows on the computer. This type of difficulty was mainly experienced in obtaining the solution for a thick L-shaped section.

For square sections the solution was obtained for different mesh sizes. Fig. 5 shows the variation of

the values of the stress function at the centre of the section with the step size. On the same graph the computational time has also been plotted for different mesh sizes. The stress function at the centre of the section has been chosen as a representative value because it has the largest magnitude and is therefore most succeptible to change with the mesh size.

From this graph it can be seen that after a certain mesh size the solution converges to a value which does not change with a decrease in the mesh size. However, the computational time increases very rapidly with the decrease in the step size.

In our problem, therefore, the most appropriate mesh size for a square section, considering the accuracy as well as economy in time, is to take about 10 to 12 meshes along the centre line OA, for the values of n less than about 20.

Similarly, for other sections also a proper mesh size may be chosen such that the method works and gives a converging solution with a minimum of computational time.

5.2 CONVERGENCE TO ELASTIC IDEALLY PLASTIC SOLUTION:

The method has been tested for convergence and accuracy, using the criterion that for large values of n

(or for large values of λ for the piecewise linear approximation), the solution should approach the elastic ideally plastic solution. That is, inside the plastic region, the resultant shear stresses should everywhere approach the yield stress $\bar{\sigma}_e = 1$.

The solution has been obtained for n = 30 with $\theta/\theta_0 = 1.5$ and 1.6. The maximum value of $\bar{\sigma}_e$ comes out to be 1.045 and 1.118 respectively. The contours of $\bar{\sigma}_e$ have been shown in Fig. (6) for $\theta/\epsilon_0 = 1.6$. From this it can be seen that over most of the plastic region, the value of $\bar{\sigma}_e$ differs from 1 by less than about 8 percent. It is felt that if n is taken still larger, then the solution will approach the elastic- ideally plastic solution even more closely. However, we have not experimented with values of n larger than 30 because of the large computational time required (more than an hour on the I.B.M.7044).

5.3 RESULTS FOR A SQUARE SECTION

The proposed numerical technique has been first tried on a square section. This case has been investigated in detail for various values of the angle of twist θ/ϵ_0 and the strain-hardening parameter n. This cross-section has also been solved for the piecewise linear stress-strain relation.

Figures (7) and (8) show the elasto-plastic boundary and the variation of $\bar{\sigma}_e$ along the central line of the section respectively, for different values of θ/θ_c. The effect of n on the elastoplastic boundary and on $\bar{\sigma}_e$ has been shown in Figs. (9) and (10). Fig. (11) shows the difference between the initial guess (obtained from the elastic solution) of the elasto-plastic boundary and the elasto-plastic boundary obtained from elasto-plastic solution. Some of the conclusions which can be drawn from these graphs are as follows:

(1) The shapes of the elasto-plastic boundaries are similare for different values of the angle of twist θ/θ_c; and they are almost parallel (see Fig. (7)).

(2) Relative to its initial position (corresponding to the first approximation based on the elastic solution), the elasto-plastic boundary does not shift along its entire length in one direction. It can be seen that over some of the portions near the centre line of the section, the elasto-plastic boundary shifts slightly into the elastic region increasing the plastic area; whereas, over the remaining major portion it shifts into the plastic region towards the free boundary of the section thereby decreasing the plastic area. In Fig. (11),

this shifting of the elasto-plastic boundary has been shown for the three values of θ/θ_o = 1.2, 1.5 and 2.0.

Fig. (9) shows that for n = 15 this change in the position of the elasto-plastic boundary is more than for n = 5, for all the three values of θ/θ_o. In fact n = 5 gives a boundary which is very close to the initial guess, obtained from the elastic solution. As n increases, this departure also becomes more and more. The nature of the shifting of the boundary remains the same as described earlier. Fig. (9) also suggests that small changes (by one or two) in the values of n will not alter the elasto-plastic boundary appreciably. Therefore,

i) For all practical purposes, for the values of θ/θ_o which are slightly more than one (1.0 to 1.25 or 1.3), it is reasonable to assume that the region of plastic deformation is more or less the same as is obtained on the basis of the elastic solution only. This will be more so for materials for which the values of n are low.

ii) For low values of n, the elasto-plastic boundary is not sensitive to changes in n.

(3) However, Fig. (10) shows that the resultant shear stress distribution within the plastic region alters appreciably with changes in the values of n, even though it does not effect the stress distribution in the elastic region. Hence the stress concentration will be different for different values of n. For example, for $\Theta/\Theta_0 = 1.5$, $\bar{\sigma}_e$ maximum (at the middle of the sides) will be 1.415 and 1.241 for n = 5 and n = 15 respectively.

As the value of n decreases, the shear stress distribution approaches the elastic solution more closely. For large values of n, the solution converges towards the elastic-ideally plastic solution.

Fig. (12) shows the contours of the shear stresses over the cross-section. It can be seen that the shape of the contours do not seem to change even after plastic deformation has taken place.

The non linear nature of the variation of the torque with the angle of twist Θ/Θ_0 has been shown in the Fig. (13). For a fixed Θ/Θ_0, the torque remains almost constant for different n.

The effect of changing the values of the parameter α in the stress-strain relation (3.4.5) has been

studied by obtaining the solution for $\Theta/\Theta_o = 1.5$ and n = 15 for $\alpha = 0.015$, 0.020 and 0.025. Fig. (14) shows the values of $\bar{\sigma}_e$ along the central line of the square section for all the three values of α. It can be seen that decreasing values of α give higher stresses in the plastic region. Though the changes in the stresses are very small for these three cases, the values of the shear stresses and the elasto-plastic boundary will be affected quite appreciably if the permanent yield strain α is taken to be very much different from 0.02 (say 0.002, as suggested by many authors).

For the piecewise linear work hardening approximation the solution has been obtained for the values of the work hardening parameter $\lambda = 6$ and 13.5 (i.e. corresponding to $E/E' = 5$ and 10).

Fig. (15) shows the elasto-plastic boundary, for $\Theta/\Theta_o = 1.5$, for $\lambda = 6$ and n = 15, along with the initial guess of the boundary obtained from the elastic solution (i.e the contour along which, in the elastic solution, $\bar{\sigma}_e = 1$. Note that for this guess the stress $\bar{\sigma}_e$ will be higher than $\bar{\sigma}_e = 1$ at many points). It can be seen that the shrinking of the elasto-plastic boundary relative to its first approximation based on elastic solution, towards

the free surface of the cross-section (decrease in plastic area), is more for the piecewise linear work hardening approximation than for the values of n around 15 in the polynomial work hardening approximation.

Fig. (16) shows the shear stress distribution along the central line of the cross-section. The maximum value of $\bar{\sigma}_e$ comes out to be as 1.087 and 1.044 for $\lambda = 6$ and 13.5 respectively. $\bar{\sigma}_e = 1.044$, being very close to one shows that over the entire plastic region the resultant shearing stresses will be very nearly equal to the yield shear stress. Hence the values of λ greater than 10 may be assumed to give a solution which approaches the elastic-ideally plastic solution closely. This inference is also consistant with the amount of shifting of the elastoplastic boundary for large values of n (See Fig. (15) for $\lambda = 6$ and compare with n = 15).

5.4 RESULTS FOR OTHER SECTIONS:

The method has also been used for the solution of rectangular and thick L - sections. For these sections the plastic zone develops around more than one point over the cross-section.

For rectangular sections, solutions have been obtained for the side's ratio of 1.2, 1.5, 2.0 and 5.0. For these four cases, Figs. (17.a), (17.b), (18) and (19) show the shape of the elasto-plastic boundary for $\epsilon/\epsilon_0 = 1.5$ and n = 15. It can be seen that the plastic region, which develops around the centre of the shorter side of the section, decreases with the increase in the side's ratio. For a fixed ϵ/ϵ_0, the shear stress concentration is not much affected by changes in the side's ratio. For example, the maximum value of $\bar{\sigma}_e$ for side's ratios of 1.2 and 5 is 1.209 and 1.193 respectively. Fig. (19) shows that for large values of the side's ratio (b/a = 5) the elasto-plastic boundary, along the longer side of the section, remains almost parallel to the free surface, over the major portion of its length.

The solution has also been obtained for two types of thick L - sections. When the solution was first attempted for the type of section shown in Fig. (20), by taking 10 meshes along the vertical edge of the section, a solution could not be obtained because of the ill conditioning of the matrix after a few iterations. The procedure was then repeated after decreasing the mesh size till it gave a converging solution (for this case 14 meshes were taken along the vertical edge of the section); however

the solution was not checked for convergence with respect to the mesh size. While obtaining the solutions for other sections, it was found that if the solution converges for a particular grid spacing then it is close to the actual solution; otherwise the solution does not converge at all; in fact for a square section the elastic-plastic boundary is hardly affected. The other type of L - section, shown in Fig. (21), has been solved for two values of n (n = 5 and n = 10). For this section, when 15 meshes were taken along the vertical edge of the section the matrix was much smaller than for the previous L - section and less computer time was required.

Therefore, it may be concluded that, for different shapes of L - sections, different types of grid spacings are required to obtain a converging solution. As a suggestion for further work, it may be of use to take a finer mesh around the point of high stress concentration where the stresses vary comparatively more abruptly; over the remaining portions of the section where the stress variation is slow, a comparatively coarser mesh will not affect the solution.

Figs. (20) and (21) show the shape of the plastic regions developed over the cross-sections of thick L - shaped sections, obtained by cutting out a square from a square, for $\Theta/\Theta_0 = 3$.

As expected, the elasto-plastic boundary near the point of maximum stress concentration suffers more change in comparision to the other regions of the cross-section undergoing plastic deformation. The shear stress concentration is affected very much by the elasto-plastic deformation. Due to this the stress distribution in the plastic region, around the point of maximum stress concentration, becomes more uniform than in the purely elastic case. The maximum value of $\bar{\sigma}_e$ for the L - section shown in Fig. (21) comes out to be 1.649 only for $\Theta/\Theta_0 = 3$ and $n = 10$.

5.5 CONCLUDING REMARKS

The numerical method which has been described in section 4, for obtaining the solution of elasto-plastic torsion problems, can be used for any other cross-section. The success of the method in obtaining the solution for the L - section shows that it is quite capable of giving the solution for sections having very high stress concentrations at some points on its boundary. The only care

that needs to be taken is to decrease the mesh size near such points of stress concentration. The greatest advantage of this technique is that it automatically takes care of all the plastic zones developed over the section and gives a solution satisfying the elastic and plastic torsion equations in their respective regions.

The method can also be used for other work - hardening laws in which $\bar{\epsilon}$ is some other polynomial function of $\bar{\sigma}_e$ i.e. $\bar{\epsilon} = f(\bar{\sigma}_e)$. It needs to be further tried for multiply connected and hollow sections.

APPENDIX - A

Diagonal systems of simultaneous linear algebraic equations have the fundamental property of being efficiently solvable by iterative methods. Among these, the Gauss - Seidel iterative method has the advantage of being simple to use. To apply this method, each equation of the system is first solved for the unknown with largest coefficient; so that the equation may be written as,

$$x_1 = a_{12} x_2 + a_{13} x_3 + \ldots\ldots a_{1n} x_n + k_1$$

$$x_2 = a_{21} x_1 + a_{23} x_3 + \ldots\ldots a_{2n} x_n + k_2$$

$$\ldots\ldots \quad \ldots\ldots \quad \ldots\ldots \quad \ldots\ldots \quad \ldots\ldots$$

$$\ldots\ldots \quad \ldots\ldots \quad \ldots\ldots \quad \ldots\ldots \quad \ldots\ldots$$

$$\ldots\ldots \quad \ldots\ldots \quad \ldots\ldots \quad \ldots\ldots \quad \ldots\ldots$$

$$x_n = a_{n1} x_1 + a_{n2} x_2 + \ldots\ldots a_{n,n-1} x_{n-1} + k_n$$

For using the iterative process, initial values $x_j^{(0)}$ for the unknowns are first assumed for starting the iterative process. New values of $x_j^{(1)}$ are then obtained from the left hand side of Eqn. (A.1). These new values $x_j^{(1)}$ are substituted in the right hand side of the equations to give the second approximation $x_j^{(2)}$. This process is continued untill $x_j^{(m)}$ is equal to $x_j^{(m+1)}$ to within the required accuracy. The $x_j^{(m)}$ are then the roots of the system.

In Gauss's method each approximation of a root is obtained by means of a single machine operation; and errors do not impair the convergence of the process since they are equivalent to a new set of starting values. The method, if convergent, converges no matter what starting values are chosen. In this method, at any stage, the best available approximation of the unknown is used in the right hand side of eqn. (A.1).

APPENDIX B

BRIEF DESCRIPTION OF THE FORTRAN PROGRAM FOR THE SOLUTION OF ELASTO-PLASTIC PROBLEM

The numerical procedure outlined previously for solving the elasto-plastic torsion problem was programmed for solution on the I.B.M. 7044 FORTRAN IV.

The correspondence between the FORTRAN symbols used in the program and the mathematical symbols employed previously is shown in the following table.

FORTRAN SYMBOL	MATHEMATICAL SYMBOL OR DESCRIPTION	FORTRAN SYMBOL	MATHEMATICAL SYMBOL OR DESCRIPTION
A	Matrix coefficients a_{ij}	THETA	Θ/Θ_0
X	Φ	YRE	$(2G\Theta)\ h^2$
DX	Φ_ξ	YRP	$(E\,\Theta)\ h^2$
DY	Φ_η	YIELD	σ_0 , σ_Y (yield stress in tension)
Y	Constant term b_i in the R.H.S. of the difference equations	H	h (mesh size)
		N,M	No of finite meshes taken along ξ or η axis.
TOW	q (resultant shear stress)		
CHI	$\bar{\sigma}e$	NP	No. of columns of the banded matrix.

FORTRAN SYMBOL	MATHEMATICAL SYMBOL OR DESCRIPTION	FORTRAN SYMBOL	MATHEMATICAL SYMBOL OR DESCRIPTION
ITURN	No. of iteration	XOLD	Values of Φ in the previous iteration.
ITURNL	Maximum or last No. of iteration	CHIOLD Or CHI1	Values of $\overline{\sigma_e}$ in the previous iteration.
AK	$(1+\nu)$		
ALFA	α		
YAN	n	KN1	Number of lowest nodal point along a vertical grid line.
TORQUE	T	KN2	Number of top nodal point along a vertical grid line

The following remarks are intended to help with the understanding of the program.

(1) Before starting the program, a net of grid lines is spread over the cross-section and the nodal points are numbered in the manner shown in Fig. (22).

(2) Subroutine ELMAT is used to write the coefficient matrix of the difference equations corresponding to the elastic torsion equation (3.6.3).

While solving such partial differential euqations by finite difference method, the coefficient matrix is banded. Hence, the coefficients of the matrix have been stored in the memory by re-stacking the band in a vertical manner. This is shown in the figure below. This procedure reduces the memory requirements.

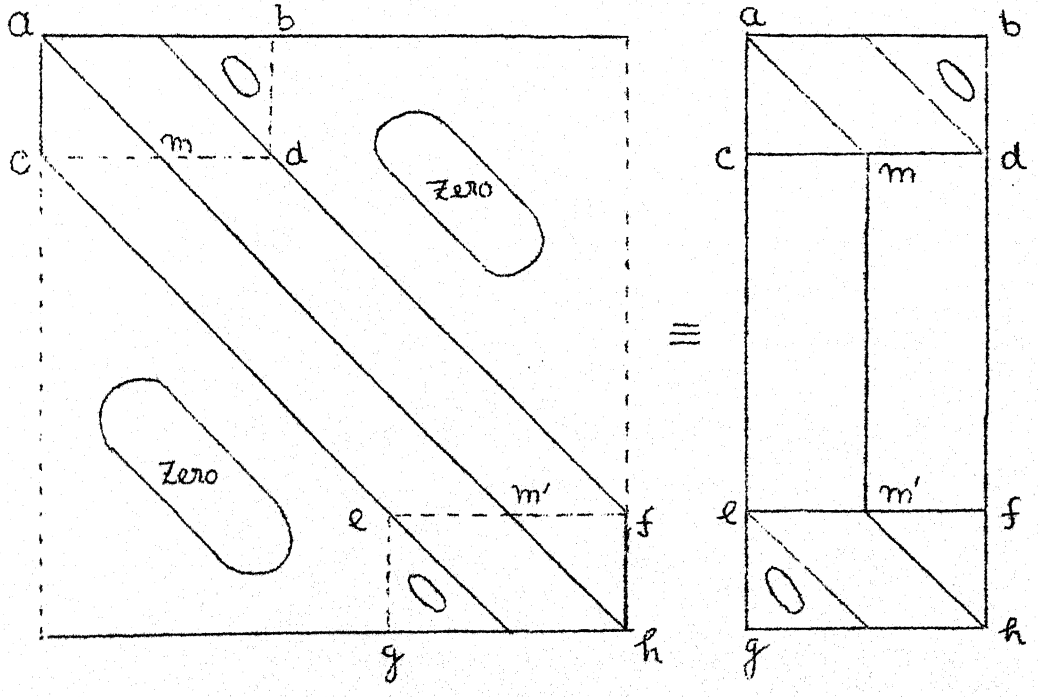

(3) Subroutine GAUSS has been written to solve the above set of simultaneous equations.

(4) Subroutine STRESS is used to calculate the effective stress $\overline{\sigma}_e$ at all the nodal points lying inside the region and at the boundary of the cross-section. For calculating $\overline{\sigma}_e$ at the boundary points, wherever necessary, partial derivatives of Φ have been computed by using one sided three or four point formulae.

(5) In going from one iteration to the next and for calculating the stresses, instead of taking the new values of Φ, the old values of Φ (from the previous iteration) are changed by a fraction of the difference between the current and the previous values. This is the reason for storing the values of Φ of the previous iteration in the memory.

(6) Subroutine PLAST has been used to modify the coefficient matrix. Every node is tested, one by, one, to check as to whether it lies in the elastic or in the plastic region. Whenever, a node point shifts from the elastic to the plastic region or from the plastic to elastic region, the corresponding difference

equation (coefficient of the matrix in that row) is re-written by using the difference equation (4.2.11) or (4.2.3) depending on whether it shifts from the elastic to the plastic region or vice-versa.

(7) Subroutine TORQ has been used for calculating the torque (T). For this the trapezoidal rule of double integration has been used.

(8) The last subroutine INTERP carries out the interpolation of the elasto-plastic boundary along every vertical as well as horizontal grid line, using the criterion that $\bar{\sigma}_e = 1$ at the elasto-plastic boundary.

FLOW DIAGRAM

A flow diagram of the procedure employed is shown on the next page.

FLOW DIAGRAM

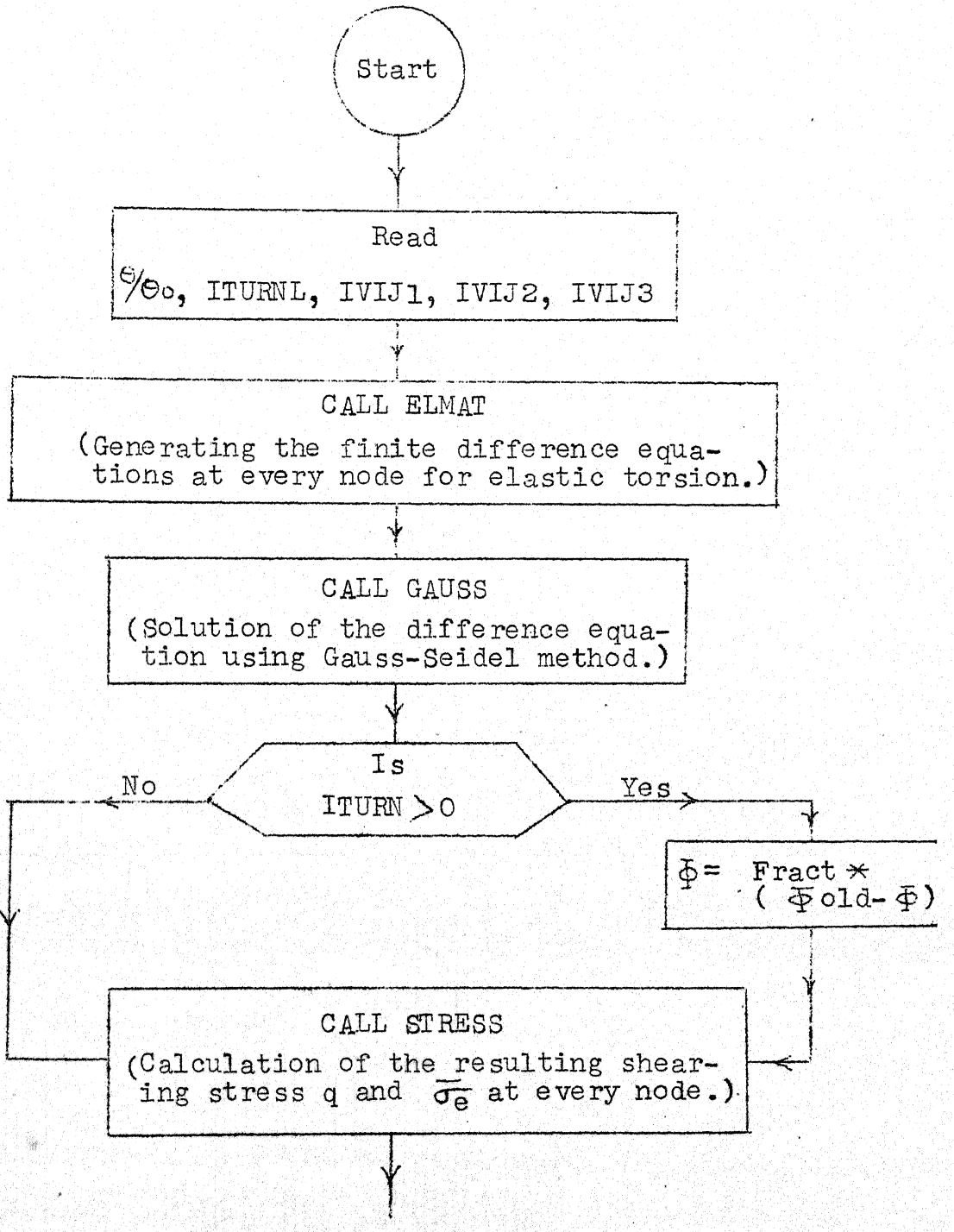

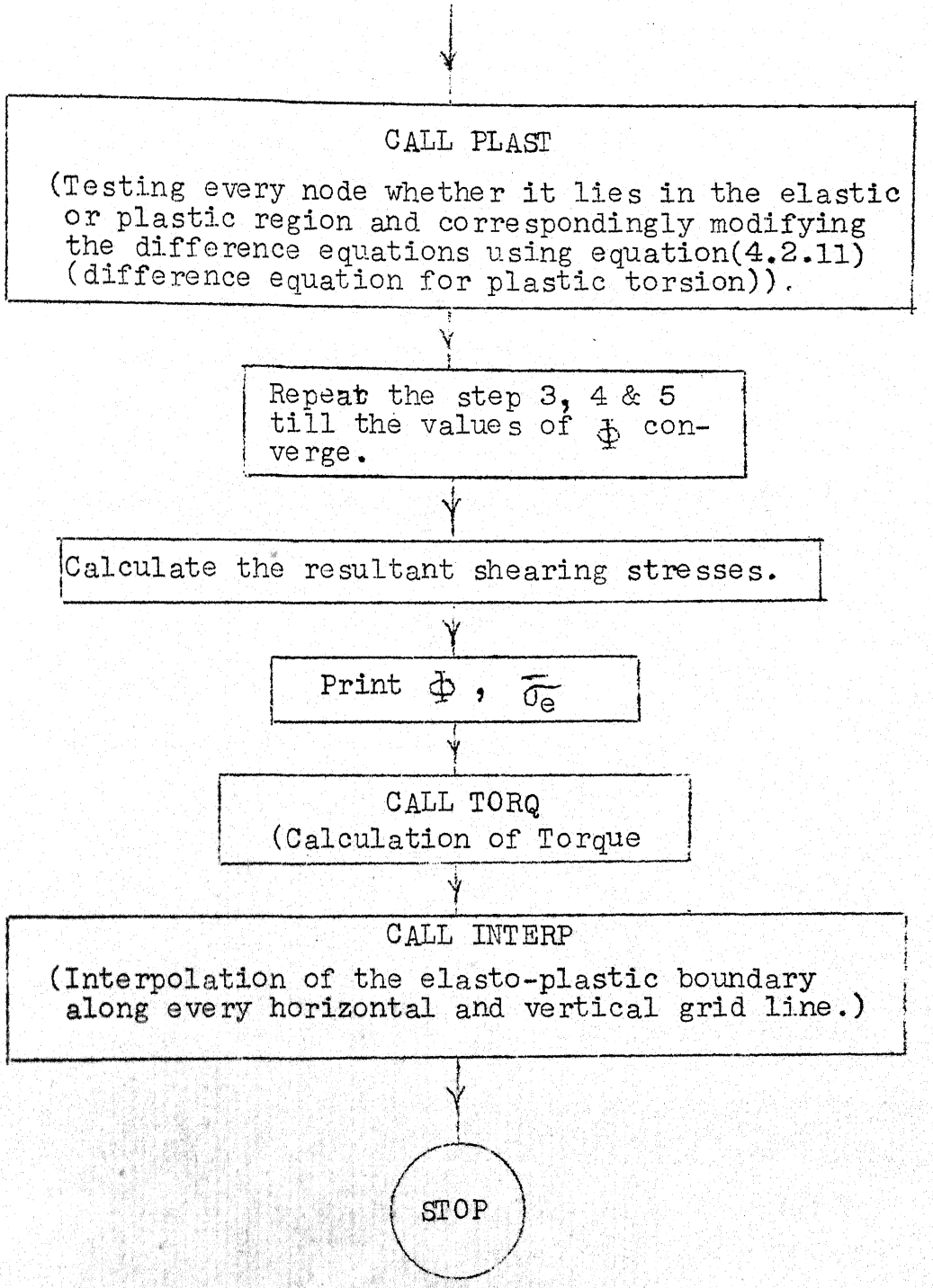
CALL PLAST
(Testing every node whether it lies in the elastic or plastic region and correspondingly modifying the difference equations using equation(4.2.11) (difference equation for plastic torsion)).
Repeat the step 3, 4 & 5 till the values of Φ converge.
Calculate the resultant shearing stresses.
Print Φ , $\bar{\sigma}_e$
CALL TORQ
(Calculation of Torque
CALL INTERP
(Interpolation of the elasto-plastic boundary along every horizontal and vertical grid line.)
STOP

APPENDIX C

```
$JOB   MEG084,TIME08,PAGES010,NAME P C UPADHYAYA
$IBJOB
$IBFTC
      ********************************************************************
      ELAST-PLASTIC SOLUTION OF A SQUARE SECTION
      ********************************************************************
      ITURN=0
      ITIN=0
      READ311,THETA,ITURNL,IVIJ1,IVIJ2,IVIJ3
      PRINT 311,THETA,ITURNL,IVIJ1,IVIJ2,IVIJ3
311   FORMAT(5X,F4.1,4(1X,I2))
      N=10
      V=N
      H=1./(2.*V)
      NL=(N**2-N)/2+N
      IP=N-1
      NP=2*IP+1
      IVIJP=IVIJ1+1
      YRE=100.
      DIMENSION A(55,19),X(55),Y(55),DX(65),DY(65),CHI(65)
      DIMENSION TOW(65),XOLD(55),CHI1(65),VERT(11),HORZ(11)
      DO 1 I=1,NL
      DO 1 J=1,NP
1     A(I,J)=0.
      DO 2 I=1,NL
2     X(I)=1000.
      DO 3 I=1,NL
3     Y(I)=YRE
      CALL ELMAT(N,NL,A,NP,IP)
351   CALL GAUSS(X,Y,A,NL,IP,NP,N,ITURN)
      IF(ITURN.EQ.1.OR.ITURN.GT.1)GO TO 111
353   PRINT 342
342   FORMAT(//50X,13HVALUES OF PHI)
      PRINT 343,(X(I),I=1,NL)
343   FORMAT(/X,8E16.6)
      CALL STRESS(X,DX,DY,NL,H,N,TOW,CHI,YRE)
      NL1=NL+1
      NL2=NL+N
      IF(ITIN.EQ.0) GO TO 600
      GO TO 660
600   YRE=YRE/CHI(NL1)*THETA
      YRP=1.25*YRE
      DO 610 I=1,NL
610   Y(I)=YRE
      DO 605 I=1,NL
605   X(I)=X(I)/CHI(NL1)*THETA
      ITIN=ITIN+1
      GO TO 353
660   PRINT 325
325   FORMAT(//40X,49HVALUES OF RESULTANT SHEAR STRESSES AT THE BOUNDRY)
      PRINT327,(TOW(I),I=NL1,NL2)
327   FORMAT(/1X,16F8.1)
      PRINT 323
```

APPENDIX C

```
£JOB    MEG084,TIME08,PAGES010,NAME P C UPADHYAYA
£IBJOB
£IBFTC
C       ***************************************************************
C
C       ELAST-PLASTIC SOLUTION OF A SQUARE SECTION
C
C       ***************************************************************
      ITURN=0
      ITIN=0
      READ311,THETA,ITURNL,IVIJ1,IVIJ2,IVIJ3
      PRINT 311,THETA,ITURNL,IVIJ1,IVIJ2,IVIJ3
 311  FORMAT(5X,F4.1,4(1X,I2))
      N=10
      V=N
      H=1./(2.*V)
      NL=(N**2-N)/2+N
      IP=N-1
      NP=2*IP+1
      IVIJP=IVIJ1+1
      YRE=100.
      DIMENSION A(55,19),X(55),Y(55),DX(65),DY(65),CHI(65)
      DIMENSION TOW(65),XOLD(55),CHI1(65),VERT(11),HORZ(11)
      DO 1 I=1,NL
      DO 1 J=1,NP
 1    A(I,J)=0.
      DO 2 I=1,NL
 2    X(I)=1000.
      DO 3 I=1,NL
 3    Y(I)=YRE
      CALL ELMAT(N,NL,A,NP,IP)
 351  CALL GAUSS(X,Y,A,NL,IP,NP,N,ITURN)
      IF(ITURN.EQ.1.OR.ITURN.GT.1)GO TO 111
 353  PRINT 342
 342  FORMAT(//50X,13HVALUES OF PHI)
      PRINT 343,(X(I),I=1,NL)
 343  FORMAT(/X,8E16.6)
      CALL STRESS(X,DX,DY,NL,H,N,TOW,CHI,YRE)
      NL1=NL+1
      NL2=NL+N
      IF(ITIN.EQ.0) GO TO 600
      GO TO 660
 600  YRE=YRE/CHI(NL1)*THETA
      YRP=1.25*YRE
      DO 610 I=1,NL
 610  Y(I)=YRE
      DO 605 I=1,NL
 605  X(I)=X(I)/CHI(NL1)*THETA
      ITIN=ITIN+1
      GO TO 353
 660  PRINT 325
 325  FORMAT(//40X,49HVALUES OF RESULTANT SHEAR STRESSES AT THE BOUNDRY)
      PRINT327,(TOW(I),I=NL1,NL2)
 327  FORMAT(/1X,16F8.1)
      PRINT 323
```

```
 323  FORMAT(//45X,34HVALUES OF RESULTANT SHEAR STRESSES)
      PRINT327,(TOW(I),I=1,NL)
      PRINT 331
      PRINT335,(CHI(I),I=NL1,NL2)
      PRINT 333
      PRINT335,(CHI(I),I=1,NL)
 331  FORMAT(//40X,27HVALUES OF SIGMA AT BOUNDARY)
 333  FORMAT(//50X,15HVALUES OF SIGMA)
 335  FORMAT(2X,16F8.3)
      IF(ITURN.EQ.0.OR.ITURN.GT.IVIJ2) GO TO 777
      GO TO 775
 777  CALL TORQ(X,H,TORQUE,N,IP)
      CALL INTERP(CHI,VERT,HORZ,IP,N,NL)
 775  DO 350 I=1,NL
 350  XOLD(I)=X(I)
      IF(ITURN.EQ.0)GO TO 361
      GO TO 367
 361  DO 363 I=1,NL
 363  CHI1(I)=CHI(I)
 367  ITURN=ITURN+1
      IF(ITURN-ITURNL)354,354,357
 354  PRINT 358
 358  FORMAT(1X,128(1H*))
      PRINT 359,ITURN
 359  FORMAT(//60X,6HITURN=,I3)
      CALL PLAST(IP,N,NL,NP,A,CHI,Y,CHI1,YRE,YRP)
      GO TO 351
 111  IF(ITURN.GT.IVIJ1) GO TO 113
      IF(ITURN.GT.IVIJ2)GO TO 115
 121  IF(ITURN.GT.IVIJ3) GO TO 119
      FRACT=0.2
      GO TO 117
 119  FRACT=0.5
      GO TO 117
 115  FRACT=0.8
      GO TO 117
 113  FRACT=1.
 117  DO 352 I=1,NL
 352  X(I)=XOLD(I)+FRACT*(X(I)-XOLD(I))
      GO TO 353
 357  CALL TORQ(X,H,TORQUE,N,IP)
      CALL INTERP(CHI,VERT,HORZ,IP,N,NL)
      STOP
      END
£IBFTC SUB1
      SUBROUTINE ELMAT(N,NL,A,NP,IP)
      DIMENSION A(NL,NP)
      A(1,1)=4.
      A(1,2)=-4.
      DO 1 I=2,IP
      A(I,I-1)=-1.
      A(I,I)=4.
      A(I,I+1)=-1.
      II=IP+I
      A(I,II)=-2.
```

```
      A(N,N-1)=-1.
      A(N,N)=4.
      NII=N+IP
      A(N,NII)=-2.
      NE=0
      KN1=N+1
      IRRO=0
      L=N
      NS=NL-IP
      N1=N-2
      DO 9 I=1,N1
      IR=I+1
      IRR=I
      IRRN=IRRO+IRR
      KN2=N*IR-IRRN
      L=L-1
      DO 2 J=KN1,KN2
      NML=N-L
      NPL=N+L
      IF(J.GT.NS)GO TO 4
      A(J,N)=4.
      IF(J.EQ.KN1)GO TO 3
      A(J,NML)=-1.
      A(J,NPL-1)=-1.
      A(J,N-1)=-1.
      IF(J.EQ.KN2)GO TO 2
      A(J,N+1)=-1.
      GO TO 2
3     A(J,NML)=-2.
      A(J,N+1)=-2.
      GO TO 2
4     NE=NE+1
      NPNE=N+NE
      NMLP=N-L+NE
      NPLP=N+L+NE
      A(J,NPNE)=4.
      IF(J.EQ.KN1) GO TO 5
      A(J,NMLP)=-1.
      A(J,NPLP-1)=-1.
      A(J,NPNE-1)=-1.
      IF(J.EQ.KN2)GO TO 2
      A(J,NPNE+1)=-1.
      GO TO 2
5     A(J,NMLP)=-2.
      A(J,NPNE+1)=-2.
2     CONTINUE
      KN1=KN2+1
      IRRO=IRRN
9     CONTINUE
      A(NL,NP)=4.
      A(NL,NP-1)=-2.
      RETURN
      END
$IBFTC SUB2
      SUBROUTINE GAUSS(X,Y,A,NL,IP,NP,N,ITURN)
```

```
      DIMENSION X(NL),Y(NL),A(NL,NP)
      IT=1
      ITL=200
      IF(ITURN.GT.1) GO TO 21
      GO TO 20
 21   ITL=75
 20   DO 60 I=1,N
      P=Y(I)
      DO 50 J=1,NP
      IF(I-J)40,50,40
 40   P=P-A(I,J)*X(J)
 50   CONTINUE
      X(I)=P/A(I,I)
 60   CONTINUE
      INC=1
      NT=N+1
      NTR=NL-IP
      DO 70 I=NT,NTR
      P=Y(I)
      DO 65 J=1,NP
      INN=INC+J
      IF(I-(INC+J))68,65,68
 68   P=P-A(I,J)*X(INN)
 65   CONTINUE
      X(I)=P/A(I,IP+1)
      INC=INC+1
 70   CONTINUE
      INC=INC-1
      NNP=NL-IP+1
      NH=N+1
      DO 90 I=NNP,NL
      P=Y(I)
      DO 80 J=1,NP
      NPP=NL-NP+J
      IF(I-(INC+J))85,80,85
 85   P=P-A(I,J)*X(NPP)
 80   CONTINUE
      X(I)=P/A(I,NH)
      NH=NH+1
 90   CONTINUE
      IT=IT+1
      IF(IT-ITL)20,20,30
 30   RETURN
      END
£IBFTC SUB3
      SUBROUTINE STRESS(X,DX,DY,NL,H,N,TOW,CHI,YRE)
      DIMENSION X(55),DX(65),DY(65),TOW(65),CHI(65)
C
C     CALCULATION OF DERIVATIVES IN Y-DIRECTION
C
      IR=N-1
      NLMT=NL-2
      LNBW1=1
      JRRO=0
      DO 1 I=1,IP
```

```
      JR=I
      JRR=I-1
      JRRN=JRRO+JRR
      LNEW2=N*JR-JRRN
      DO 2 J=LNEW1,LNEW2
      IF(J.EQ.LNEW1)GO TO 3
      IF(J.EQ.LNEW2)GO TO 4
      DY(J)=(X(J-1)-X(J+1))/(2.*H)
      GO TO 2
 3    IF(J.EQ.NLMT)GO TO 5
      IF(J.EQ.1)GO TO 6
      DY(J)=(3.*X(J)-4.*X(J+1)+X(J+2))/(2.*H)
      GO TO 2
 4    DY(J)=(X(J-1)-0.)/(2.*H)
      GO TO 2
 5    DY(J)=(3.*X(J)-4.*X(J+1))/(2.*H)
      GO TO 2
 6    DY(1)=0.
 2    CONTINUE
      LNEW1=LNEW2+1
      JRRO=JRRN
 1    CONTINUE
      DY(NL)=(3.*X(NL)-4.*X(NL-1)+X(NL-3))/(2.*H)
      NEX1=NL+1
      NEX2=NL+N-1
      K=N
      J=0
      DO 15 I=NEX1,NEX2
      J=J+K
      DY(I)=-(4.*X(J)-X(J-1))/(2.*H)
 15   K=K-1
      NLPN=NL+N
      DY(NLPN)=-(YRE+X(NL))/(2.*H)
C
C      CALCULATION OF DERIVATIVES IN X-DIRECTION
C
 23   DX(I)=0.
      DO 25 I=NEX1,NLPN
 25   DX(I)=0.
      LNEW1=N+1
      JRRO=0
      LS=N
      NMT=N-2
      DO 27 I=1,NMT
      JR=I+1
      JRR=I
      JRRN=JRRO+JRR
      LNEW2=N*JR-JRRN
      LS=LS-1
      DO 29 J=LNEW1,LNEW2
      IF(J.EQ.LNEW1)GO TO 31
      JMLS=J-LS
      JPLS=J+LS
      DX(J)=(X(JMLS)-X(JPLS-1))/(2.*H)
      GO TO 29
```

```
 31    DX(J)=DY(J)
 29    CONTINUE
       LNEW1=LNEW2+1
       JRRO=JRRN
 27    CONTINUE
       DX(NL)=DY(NL)
C      CALCULATION OF SIGMA AT DIFFERENT POINTS
       YIELD=35000.
       DO 33 I=1,NLPN
 33    CHI(I)=3.**0.5*(DX(I)**2+DY(I)**2)**0.5/YIELD
       DO 35 I=1,NLPN
 35    TOW(I)=(DX(I)**2+DY(I)**2)**0.5/1.
       RETURN
       END
$IBFTC SUB4
       SUBROUTINE PLAST(IP,N,NL,NP,A,CHI,Y,CHI1,YRE,YRP)
       DIMENSION A(NL,NP),CHI(65),Y(NL),CHI1(65)
       AK=1.25
       YAN=5.
       ALFA=0.02
       DO 1 I=1,IP
       II=IP+I
       IF(CHI(I)-1.)11,11,52
 11    IF(CHI1(I).LT.1.)GO TO 1
       Y(I)=YRE
       A(I,I-1)=-1.
       A(I,I+1)=-1.
       A(I,II)=-2.
       A(I,I)=4.
       GO TO 1
 52    CONS1=AK+1.5*ALFA*(2.-YAN)*(CHI(I)**(YAN-1.))
       CONS2=1.5*ALFA*(YAN-1.)*(CHI(I)**(YAN-2.))
       Y(I)=YRP
       A(I,I-1)=-(1.*CONS1+CONS2*(CHI(I)+CHI(I-1))/2.)
       A(I,I+1)=-(1.*CONS1+CONS2*(CHI(I)+CHI(I+1))/2.)
       A(I,II)=-(1.*CONS1+CONS2*(CHI(I)+CHI(II))/2.)*2.
       A(I,I)=-(A(I,I-1)+A(I,I+1)+A(I,II))
 1     CONTINUE
       CONS1=AK+1.5*ALFA*(2.-YAN)*(CHI(N)**(YAN-1.))
       CONS2=1.5*ALFA*(YAN-1.)*(CHI(N)**(YAN-2.))
       A(N,N-1)=-(1.*CONS1+CONS2*(CHI(N)+CHI(N-1))/2.)
       NPIP=N+IP
       A(N,NPIP)=-(1.*CONS1+CONS2*(CHI(N)+CHI(NPIP))/2.)*2.
       EXTRA=-(1.*CONS1+CONS2*(CHI(N)+CHI(NL+1))/2.)
       A(N,N)=-(A(N,N-1)+A(N,NPIP)+EXTRA)
       Y(N)=YRP
       KN1=N+1
       IRRO=0
       L=N
       NS=NL-IP
       N1=N-2
       DO 9 I=1,N1
       IR=I+1
       IRRN=IRRO+I
       KN2=N*IR-IRRN
```

```
      L=L-1
      NML=N-L
      NPL=N+L
      NLPIR=NL+IR
      DO 2 J=KN1,KN2
      JML=J-L
      JPL=J+L
      IF(CHI(J)-1.)12,53,53
12    IF(CHI1(J).LT.1.)GO TO 2
      Y(J)=YRE
      IF(J.GT.NS)GO TO 14
      A(J,N)=4.
      IF(J.EQ.KN1) GO TO 13
      A(J,N-1)=-1.
      A(J,NML)=-1.
      A(J,NPL-1)=-1.
      IF(J.EQ.KN2)GO TO 2
      A(J,N+1)=-1.
      GO TO 2
13    A(J,N+1)=-2.
      A(J,NML)=-2.
      GO TO 2
14    NE=J-NS
      NPNE=N+NE
      NMLP=N-L+NE
      NPLP=N+L+NE
      A(J,NPNE)=4.
      IF(J.EQ.KN1) GO TO 15
      A(J,NPNE-1)=-1.
      A(J,NMLP)=-1.
      A(J,NPLP-1)=-1.
      IF(J.EQ.KN2)GO TO 2
      A(J,NPNE+1)=-1.
      GO TO 2
15    A(J,NPNE+1)=-2.
      A(J,NMLP)=-2.
      GO TO 2
53    CONS1=AK+1.5*ALFA*(2.-YAN)*(CHI(J)**(YAN-1.))
      CONS2=1.5*ALFA*(YAN-1.)*(CHI(J)**(YAN-2.))
      Y(J)=YRP
      IF(J.GT.NS)GO TO 4
      IF(J.EQ.KN1) GO TO 19
      A(J,N-1)=-(1.*CONS1+CONS2*(CHI(J)+CHI(J-1))/2.)
      A(J,NML)=-(1.*CONS1+CONS2*(CHI(J)+CHI(JML))/2.)
      A(J,NPL-1)=-(1.*CONS1+CONS2*(CHI(J)+CHI(JPL-1))/2.)
      IF(J.EQ.KN2) GO TO 3
      A(J,N+1)=-(1.*CONS1+CONS2*(CHI(J)+CHI(J+1))/2.)
      A(J,N)=-(A(J,N-1)+A(J,N+1)+A(J,NML)+A(J,NPL-1))
      GO TO 2
3     EXTRA=-(1.*CONS1+CONS2*(CHI(J)+CHI(NLPIR))/2.)
      A(J,N)=-(A(J,N-1)+A(J,NML)+A(J,NPL-1)+EXTRA)
      GO TO 2
19    A(J,N+1)=-(1.*CONS1+CONS2*(CHI(J)+CHI(J+1))/2.)*2.
      A(J,NML)=-(1.*CONS1+CONS2*(CHI(J)+CHI(JML))/2.)*2.
      A(J,N)=-(A(J,N+1)+A(J,NML))
```

```
      GC TO 2
 4    NE=J-NS
      NPNE=N+NE
      NMLP=N-L+NE
      NPLP=N+L+NE
      IF(J.EQ.KN1) GC TO 21
      A(J,NPNE-1)=-(1.*CONS1+CONS2*(CHI(J)+CHI(J-1))/2.)
      A(J,NMLP)=-(1.*CONS1+CONS2*(CHI(J)+CHI(JML))/2.)
      A(J,NPLP-1)=-(1.*CONS1+CONS2*(CHI(J)+CHI(JPL-1))/2.)
      IF(J.EQ.KN2) GC TO 5
      A(J,NPNE+1)=-(1.*CONS1+CONS2*(CHI(J)+CHI(J+1))/2.)
      A(J,NPNE)=-(A(J,NPNE-1)+A(J,NPNE+1)+A(J,NPLP-1)+A(J,NMLP))
      GC TO 2
 5    EXTRA=-(1.*CONS1+CONS2*(CHI(J)+CHI(NLPIR))/2.)
      A(J,NPNE)=-(A(J,NPNE-1)+A(J,NPLP-1)+A(J,NMLP)+EXTRA)
      GC TO 2
 21   A(J,NMLP)=-(1.*CONS1+CONS2*(CHI(J)+CHI(JML))/2.)*2.
      A(J,NPNE+1)=-(1.*CONS1+CONS2*(CHI(J)+CHI(J+1))/2.)*2.
      A(J,NPNE)=-(A(J,NMLP)+A(J,NPNE+1))
 2    CONTINUE
      KN1=KN2+1
      IRRO=IRRN
 9    CONTINUE
      RETURN
      END
£IBFTC SUB5
      SUBROUTINE TORQ(X,H,TORQUE,N,IP)
      DIMENSION X(55)
      TCRQUE=0.5*X(1)+2.*X(2)
      DC 1 I=3,N
 1    TCRQUE=TORQUE+2.*X(I)
      KN1=N+1
      IRRO=C
      DC 2 I=1,IP
      IR=I+1
      IRRN=IRRC+I
      KN2=N*IR-IRRN
      DC 3 J=KN1,KN2
      IF(J.EQ.KN1)GO TO 4
      KNP1=KN1+1
      IF(J.EQ.KNP1)GO TO 5
      TCRQUE=TORQUE+4.*X(J)
      GO TO 3
 4    TORQUE=TORQUE+2.*X(J)
      GC TO 3
 5    TCRQUE=TORQUE+4.*X(J)
 3    CONTINUE
      KN1=KN2+1
      IRRO=IRRN
 2    CONTINUE
      TORQUE=TORQUE*H**2/4.*8.
      PRINT 370,TORQUE
 370  FORMAT(///45X,*TORQUE=*,F12.3)
      RETURN
      END
```

```
£IBFTC SUB6
      SUBROUTINE INTERP(CHI,VERT,HORZ,IP,N,NL)
      DIMENSION CHI(65),VERT(11),HORZ(11)
C
C     INTERPOLATION ON VERTICAL LINES
C
      KN1=1
      JRRO=0
      DO 1 I=1,IP
      JRR=I-1
      JRRN=JRRO+JRR
      KN2=N*I-JRRN
      NLPI=NL+I
      IF(CHI(NLPI).LT.1.)GO TO 2
      IF(CHI(NLPI).EQ.1.)GO TO 3
      J=KN2
      V=0.
 4    IF(CHI(J).LT.1.)GO TO 5
      IF(CHI(J).EQ.1.)GO TO 6
      J=J-1
      V=V+1.
      GO TO 4
 6    VERT(I)=0.
      GO TO 2
 3    VERT(I)=0.
      GO TO 2
 5    IF(J.EQ.KN2)GO TO 21
      VERT(I)=V+(CHI(J+1)-1.)/(CHI(J+1)-CHI(J))
      GO TO 2
 21   VERT(I)=V+(CHI(NLPI)-1.)/(CHI(NLPI)-CHI(J))
 2    KN1=KN2+1
      JRRO=JRRN
 1    CONTINUE
C
C     INTERPOLATION ON HORIZONTAL LINES
C
      NP=N+1
      DO 7 I=2,NP
      IF(I.EQ.NP)GO TO 13
      L=IP
      J=I
      IF(CHI(I).LT.1.0.OR.CHI(I).EQ.1.0)GO TO 7
      H=0.
 11   JB=J
      J=J+L
      IF(CHI(J).LT.1.)GO TO 9
      IF(CHI(J).EQ.1.)GO TO 8
      L=L-1
      H=H+1.
      GO TO 11
 9    HORZ(I)=H+(CHI(JB)-1.)/(CHI(JB)-CHI(J))
      GO TO 7
 8    HORZ(I)=H+1.
      GO TO 7
 13   J=NL+2
```

```
      H=0.
 15   IF(CHI(J).LT.1.)GO TO 17
      IF(CHI(J).EQ.1.)GO TO 19
      J=J+1
      H=H+1.
      GO TO 15
 19   HORZ(I)=H+1.
      GO TO 7
 17   HORZ(I)=H+(CHI(J-1)-1.)/(CHI(J-1)-CHI(J))
 7    CONTINUE
      PRINT425
 425  FORMAT(//35X,*VERTICAL DISTANCES OF THE BOUNDRY*)
      PRINT430,(VERT(I),I=1,IP)
 430  FORMAT(/1X,15F8.3)
      PRINT435
 435  FORMAT(//35X,*HORIZONTAL DISTANCES OF THE BOUNDRY*)
      PRINT439,(HORZ(I),I=2,NP)
 439  FORMAT(/1X,16F8.3)
      RETURN
      END
£ENTRY
```

BIBLIOGRAPHY

1. Nadai, A., 'Der Beginn des Fliessvorganges in einem tortierten Stab', Z. angew. Math. Mech. 3, p. 442, (1923)

2. Christopherson, D.G., 'A theoretical investigation of plastic torsion in an I - beam', Trans. A.S.M.E., Vol. 62, p. A-1, (1940)

3. Chirstopherson, D.G. and Southwell, R.V., 'Relaxation methods applied to Engineering problems III: Problems involving two variables', Proc. Roy. Soc. A., 168, p. 317, (1938)

4. Shaw, F.S., 'The torsion of hollow and solid prism in the elastic and plastic range by relaxation methods', Aust. Counc. for Aero., ACA - 11, (1944)

5. Sokolovsky, W.W., "On a problem of Elasto-plastic torsion", P.M.M., - 6, p. 241 - 246, (1942)

6. Sokolovsky, W.W., 'Elasto-plastic torsion of a conical bar.' P.M.M. - 7, (1943)

7. Eddy, R.P. and Shaw, F.S., 'Numerical solution of Elasto-plastic torsion of a shaft of rotational symmetry', J. App. Mech., 16, p. 139 - 148 (1949)

8. Walsh, J.B. and Mackenzie, A.C., 'Elastic-plastic torsion of a circumferentially notched bar', J. Mech. Phys. Solids, Vol. 7, p. 247, (1957)

9. Hult, J.A.H., 'Elastic plastic torsion of sharply notched bars', J. Mech. Phys. Solids, Vol. 6, p. 79, (1958)

10. Rushton, K.R., 'Electrical analogue solution of elastic-plastic torsion for shaft containing structural discontinuities', J. Mech. Phys. Solids, Vol. 11, p. 269, (1963)

11. Budianskey, B., 'A reassessment of Deformation theories of plasticity', J. App. Mech., Vol. 26, p. 259, (1959)

12. Huth, J.H., 'A note on plastic torsion', J. App. Mech. Vol. 22, p. 432 - 4, (1955)

13. Greenberg, H.J., Dorn, W.S., and Wetherell, E.H., 'A comparision of flow and Deformation theories in plastic torsion of a square cylinder', Plasticity: Proceedings of the second symposium on Naval Structural Mechanics, Brown University, R.I., (1960)

14. Ramberg, W. and Osgood, W., 'Description of Stress-Strain curves by three parameters", NACA TN No. 902, July (1943)

15. Nadai, A., 'Theory of flow and fracture of solids', Vol. 1, McGraw Hill, New York, (1950)

16. Shaw, F.S., 'An Introduction to Relaxation methods' Dover Publications Inc., (1953)

17. Hill, R., 'The mathematical theory of Plasticity', O.U.P., (1950 b)

18. Drucker, D.C., 'A more fundamental approach to plastic stress-strain relations', A.S.M.E, p. 487, (1951)

19. Prager, W., 'Strain Hardening under combined stresses', J. App. Phys., Vol. 16, p. 837, (1945)

20. Hutchinson, J.W., 'Singular behaviour at the end of a tensile crack in a hardening material', J. Mech. Phys. Solids, Vol. 16, p. 13 - 31, (1968)

21. Salvadori, M.G. and Baron, M.L., 'Numerical methods in Engineering', Prentice Hall.

22. Forsythe, G.E. and Wasow, W.R., 'Finite difference methods for Partial Differential Equations', John Wiley, New York (1960)

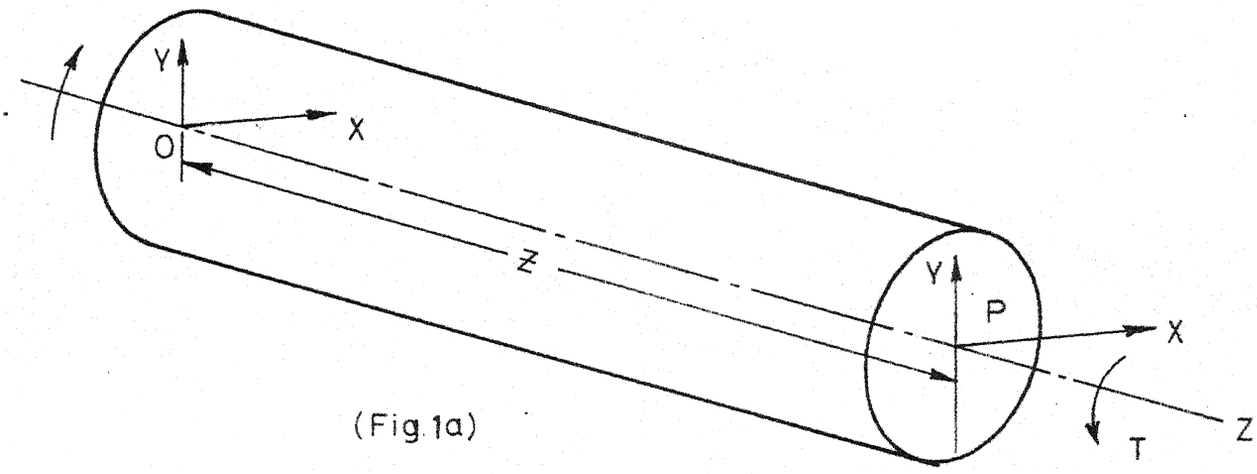

(Fig.1a)

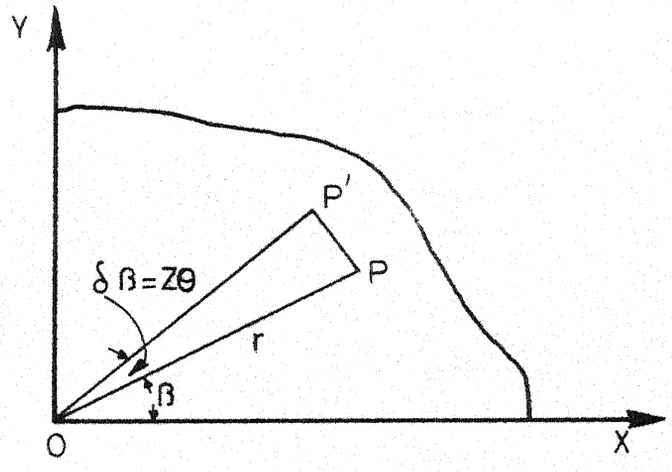

(Fig. 1b)

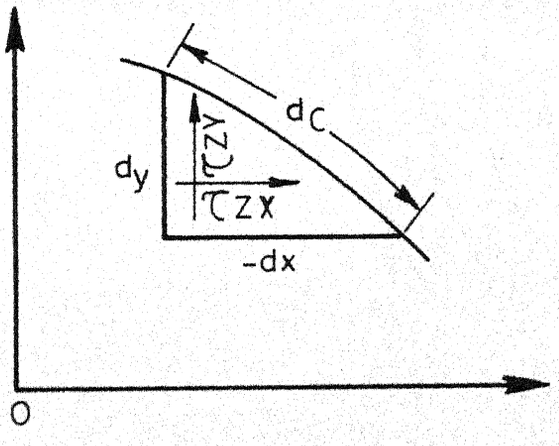

(Fig. 1c)

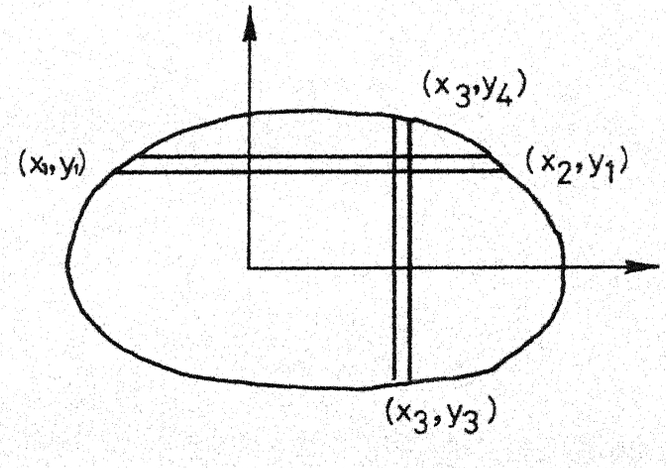

(Fig. 1d)

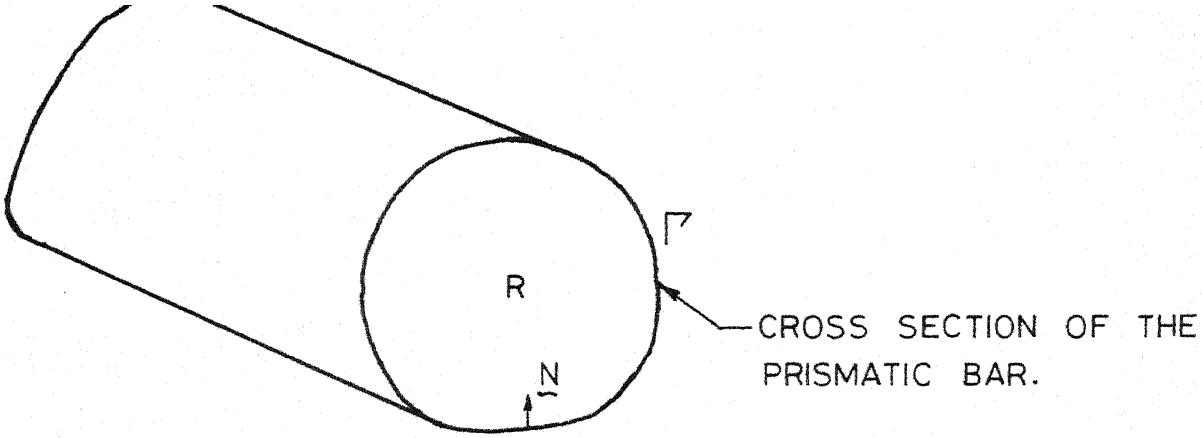

(Fig. 2a)

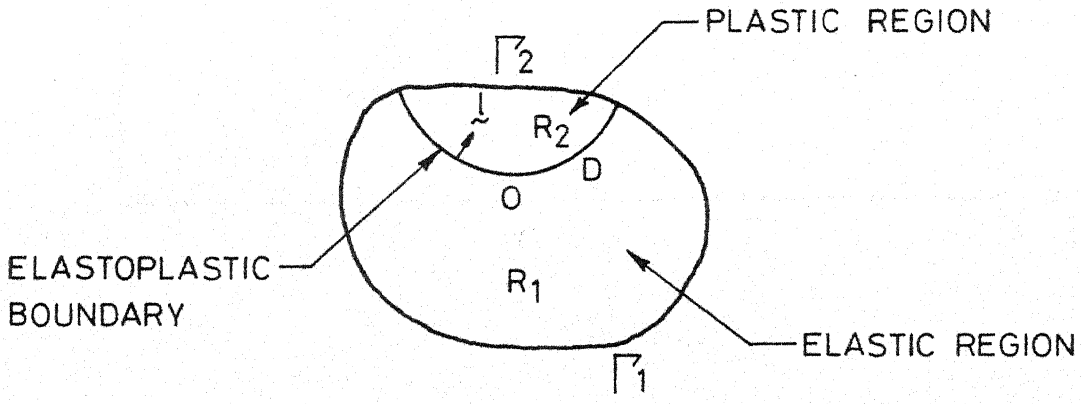

(Fig. 2b)

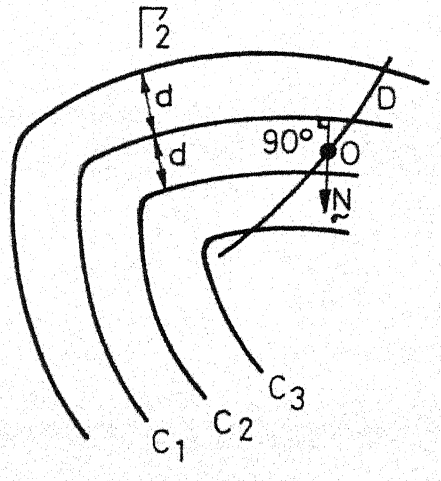

(Fig. 2c)

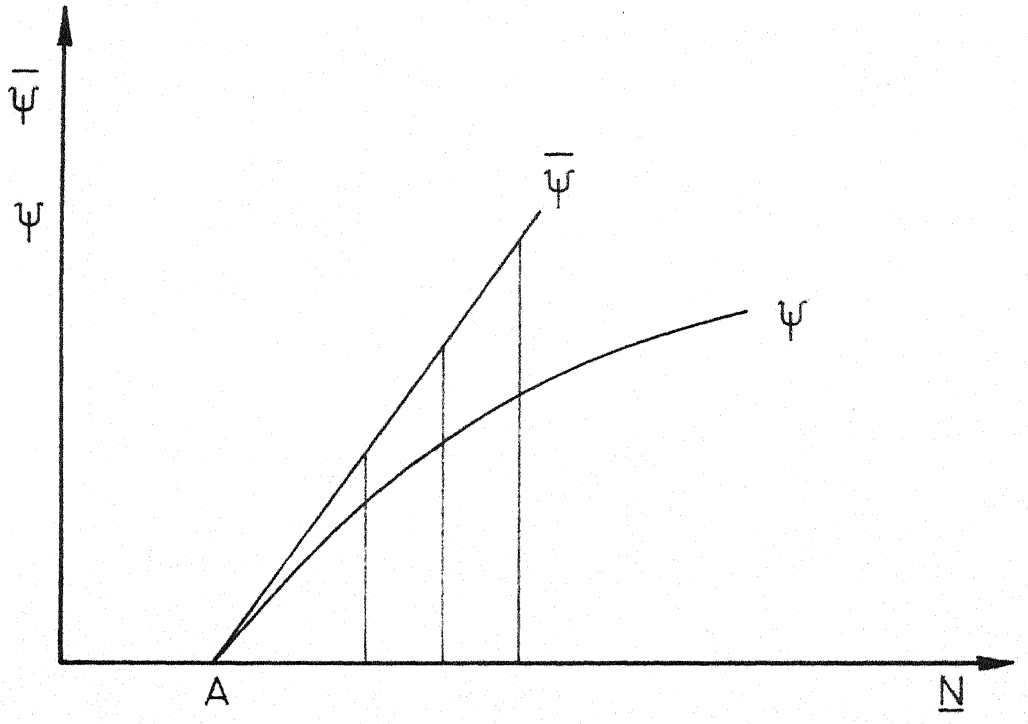
$\bar{\psi}$
ψ
$\bar{\psi}$
ψ
A
N

(Fig. 3a)

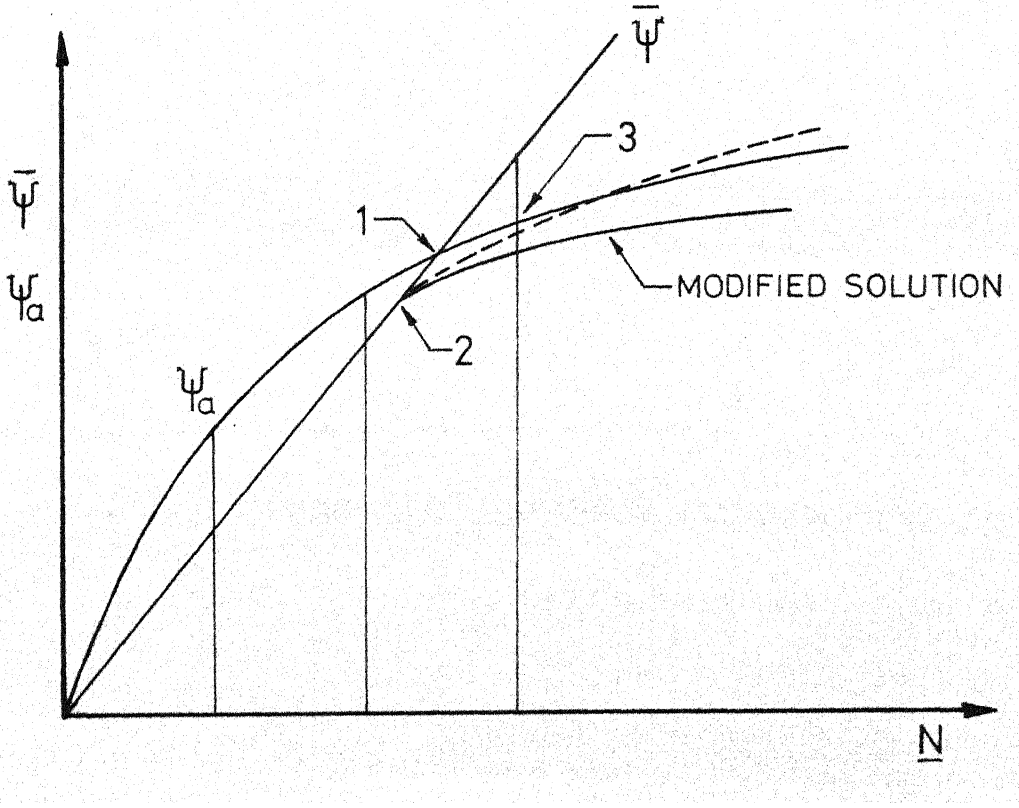
$\bar{\psi}$
$\bar{\psi}$
ψ_a
ψ_a
1
2
3
MODIFIED SOLUTION
N

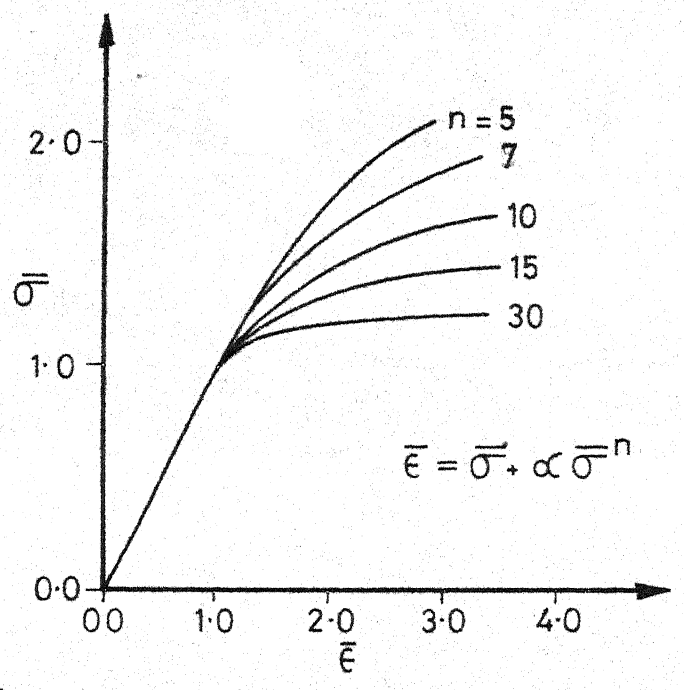

(Fig. 4a) RAMBERG-OSGOOD TYPE STRESS-STRAIN RELATION.

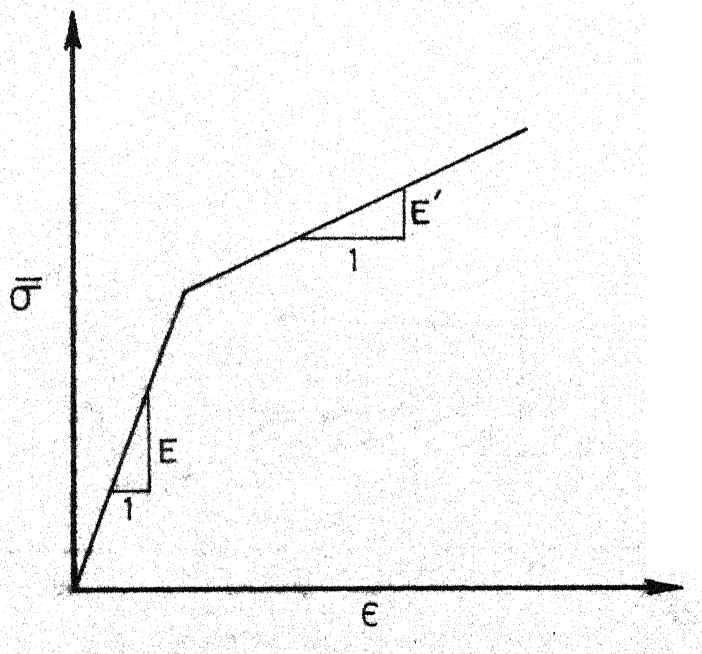

(Fig. 4b) PIECE-WISE LINEAR STRESS-STRAIN CURVE.

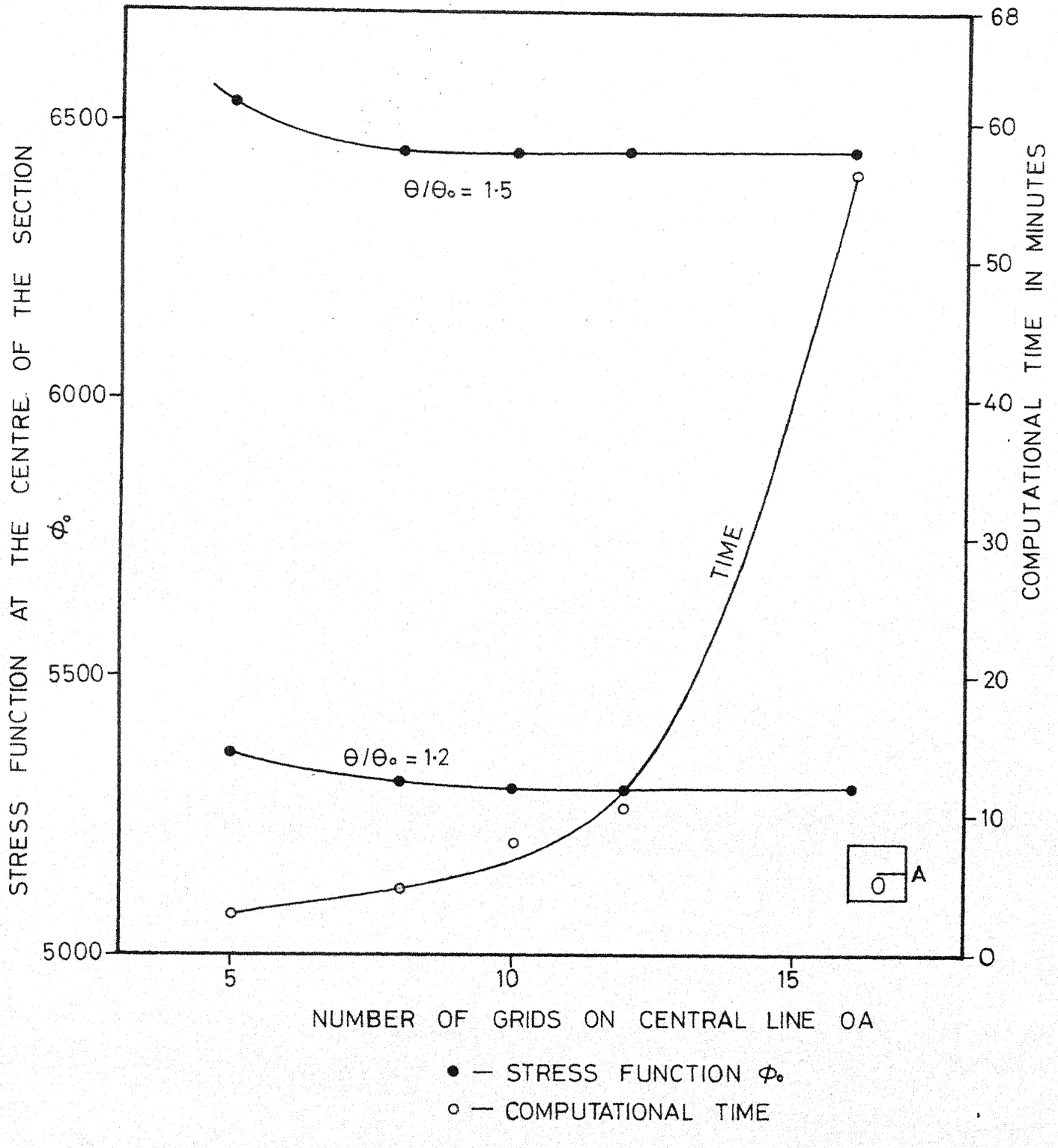

(Fig. 5) EFFECT OF MESH-SIZE FOR A RECTANGULAR SECTION.

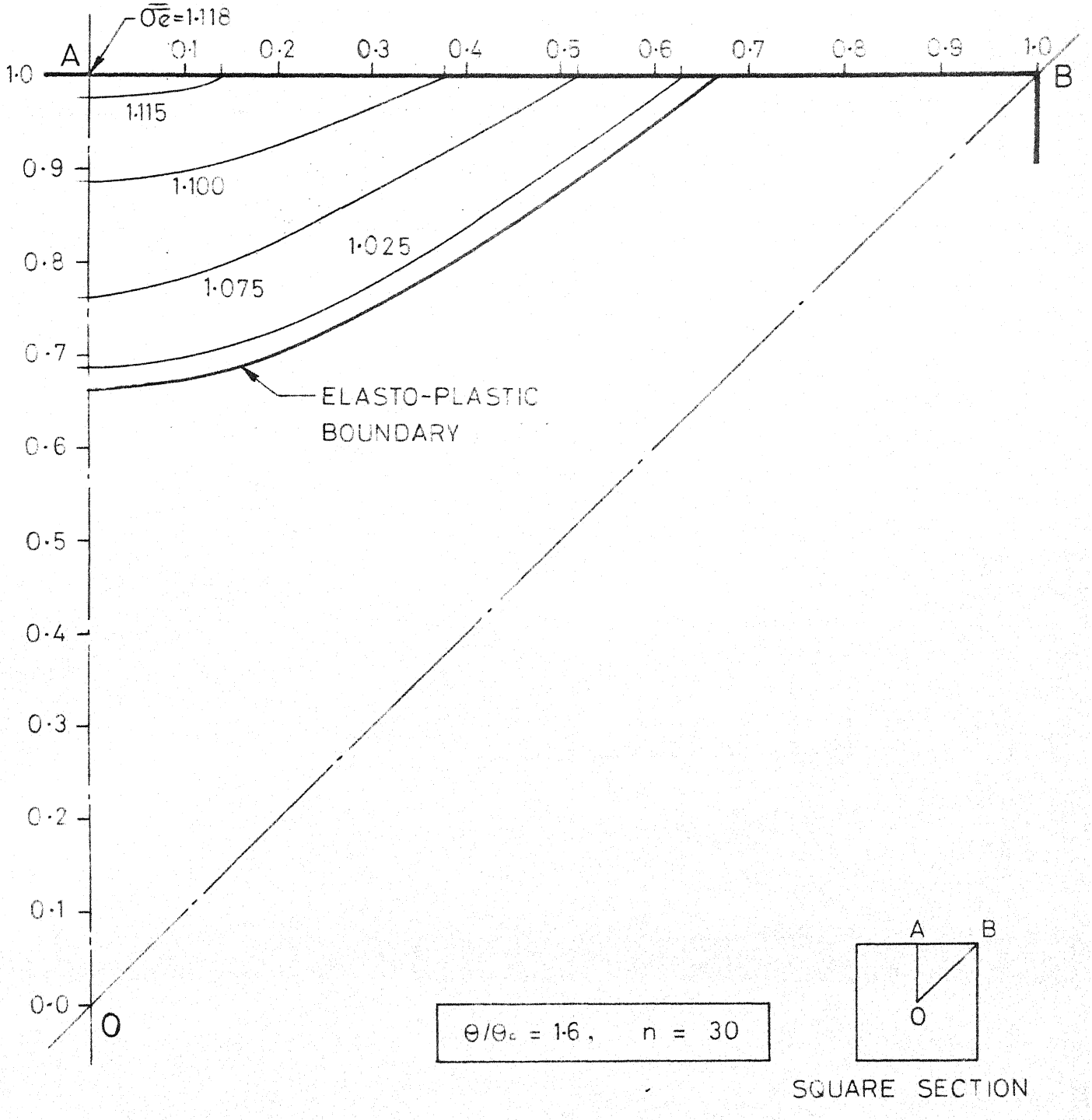

(Fig. 6) CONTOURS OF SHEAR STRESS $\overline{\sigma e}$ IN THE PLASTIC REGION.

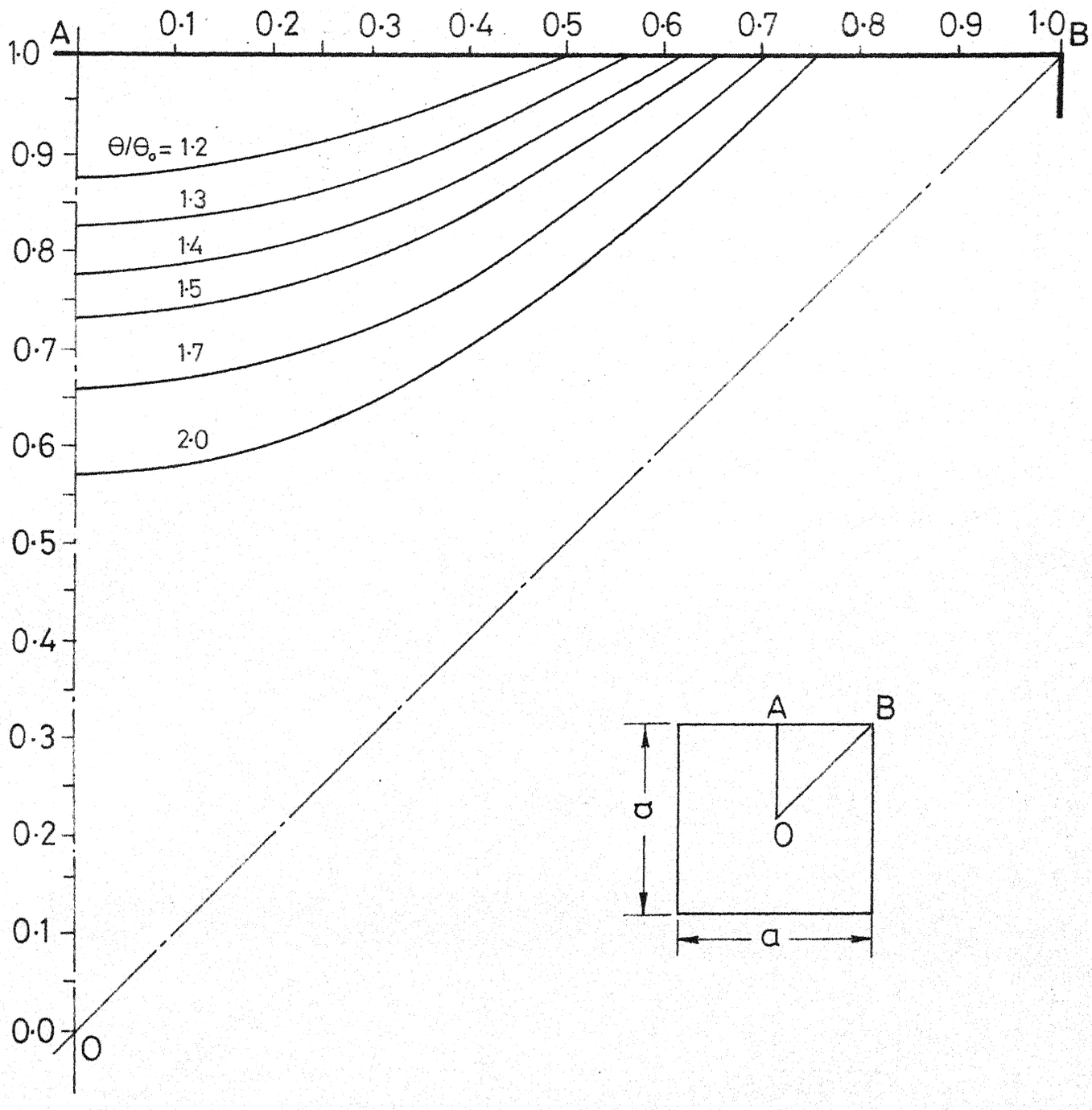

(Fig. 7) ELASTO-PLASTIC BOUNDARIES OF A SQUARE SECTION FOR DIFFERENT ANGLE OF TWIST θ/θ_0 AND $n = 15$.

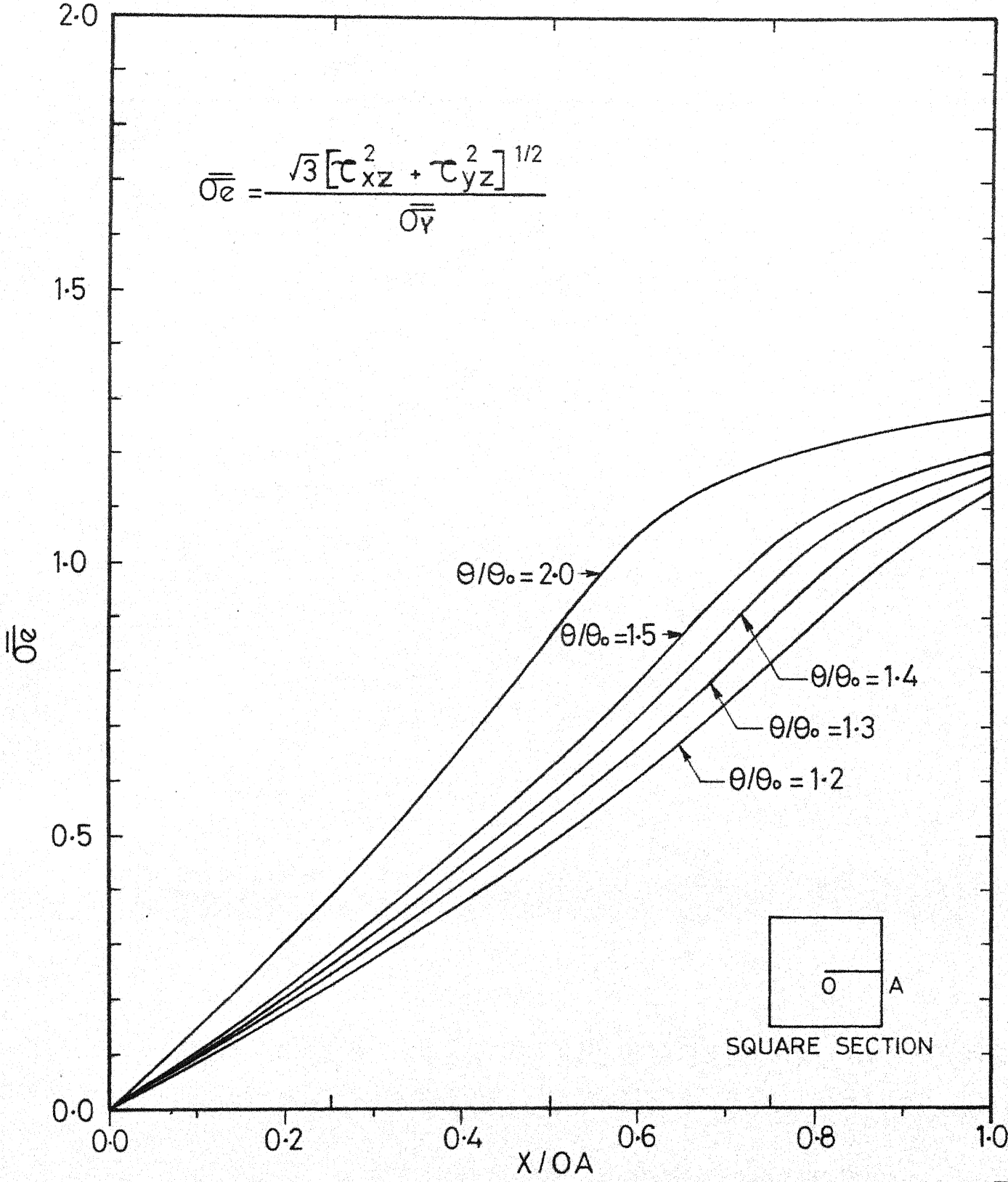

(Fig. 8) VALUES OF THE NON-DIMENSIONAL STRESS $\bar{\sigma}_e$ ALONG THE CENTRE LINE OA OF A SQUARE SECTION, FOR $n = 15$.

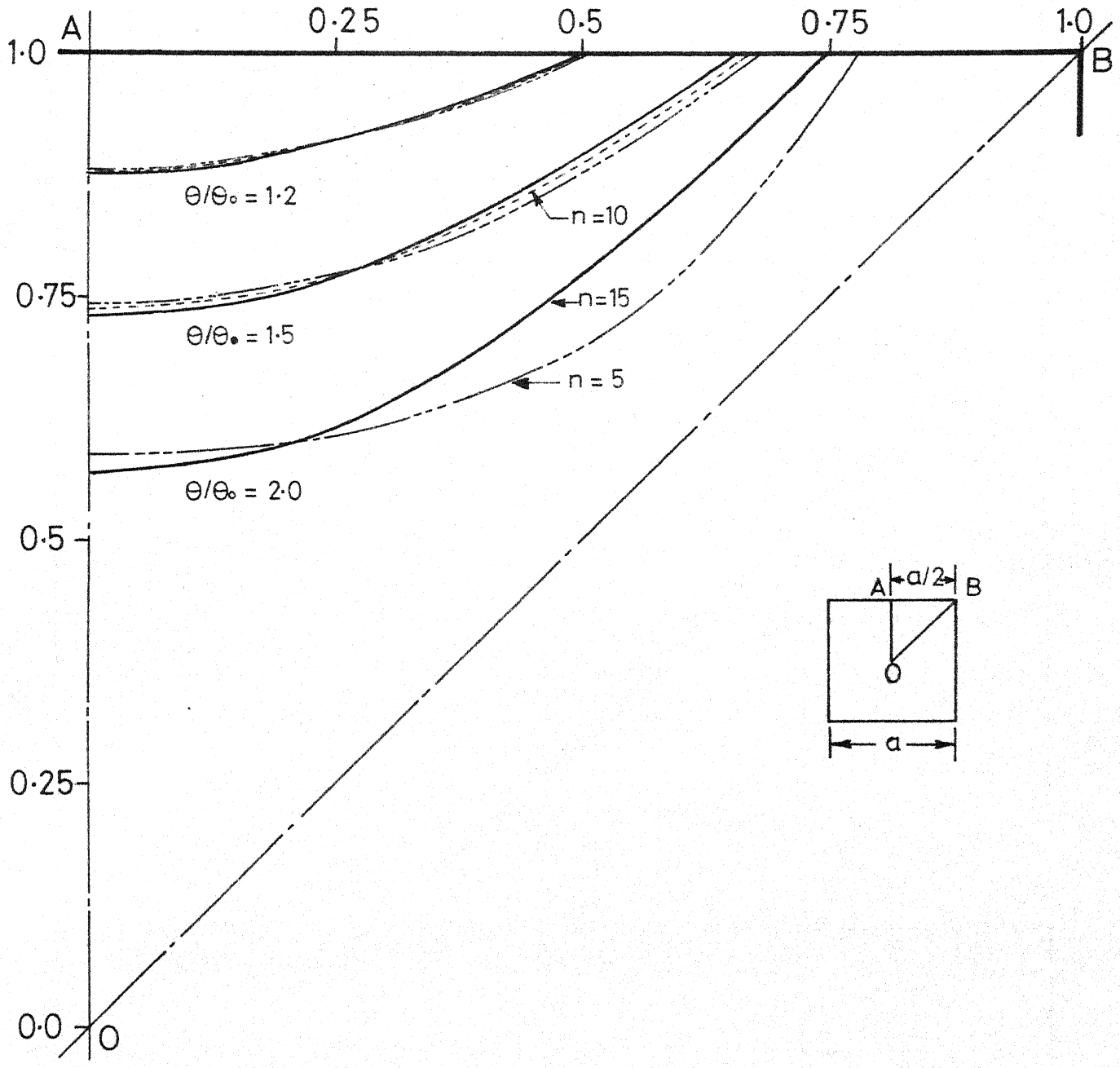

(Fig. 9) ELASTO-PLASTIC BOUNDARIES OF A SQUARE SECTION FOR DIFFERENT VALUES OF n.

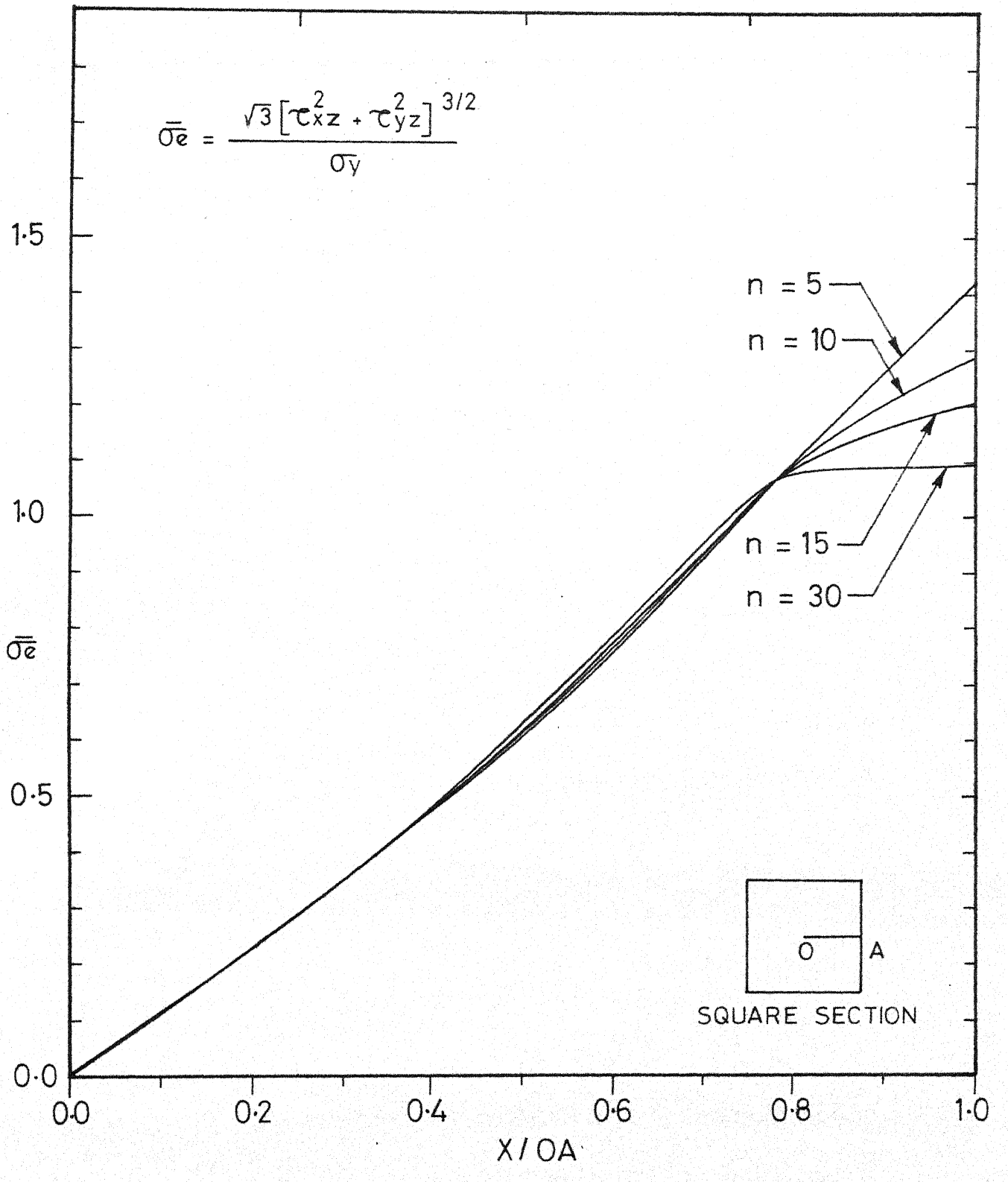

(Fig. 10) NON - DIMENSIONAL STRESS, $\bar{\sigma e}$ ALONG THE CENTRE LINE OA FOR DIFFERENT VALUES OF n AND $\Theta/\Theta_o = 1{\cdot}5$.

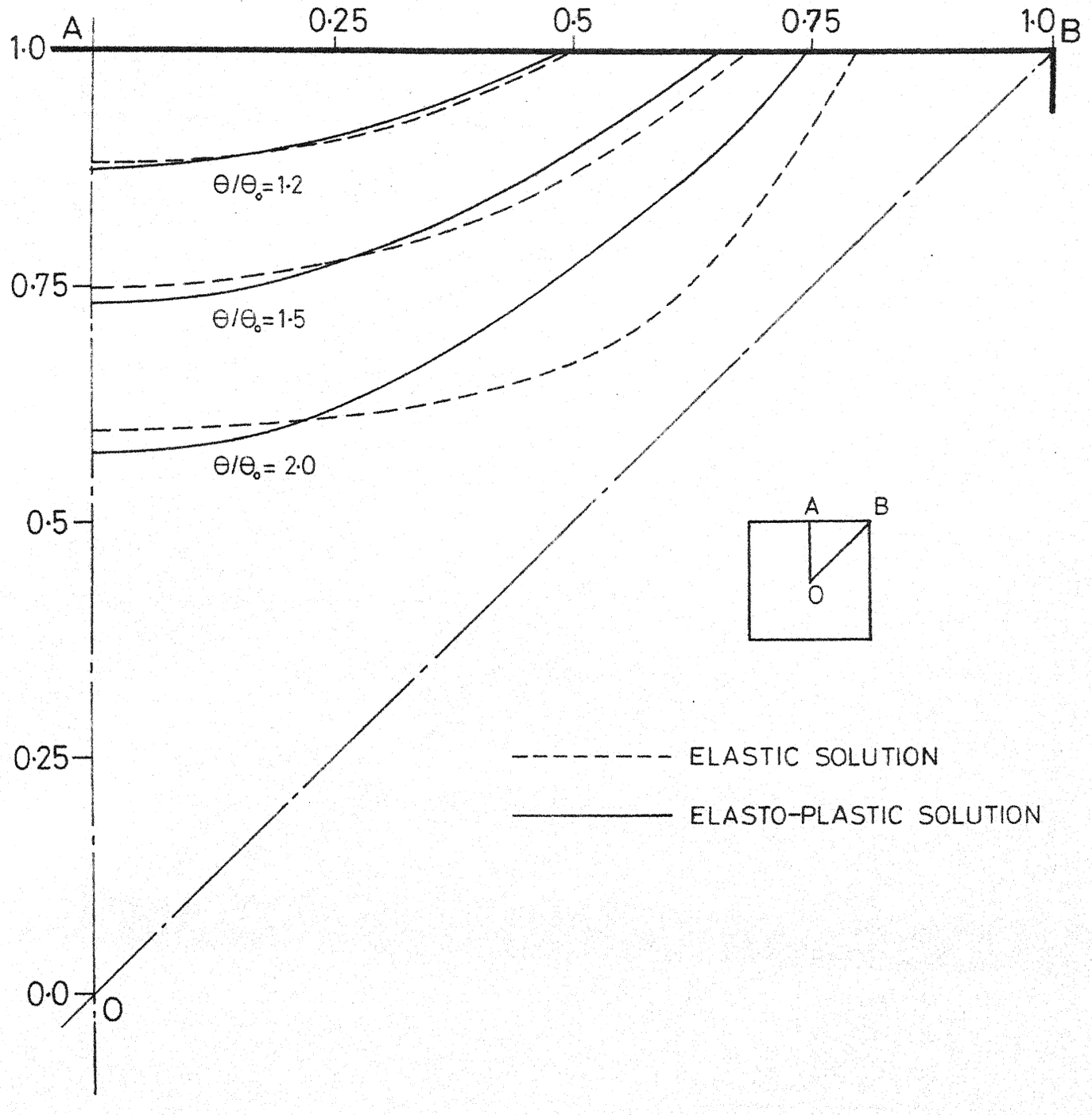

(Fig. 11.) ELASTO-PLASTIC BOUNDARY OF A SQUARE SECTION FOR n = 15.

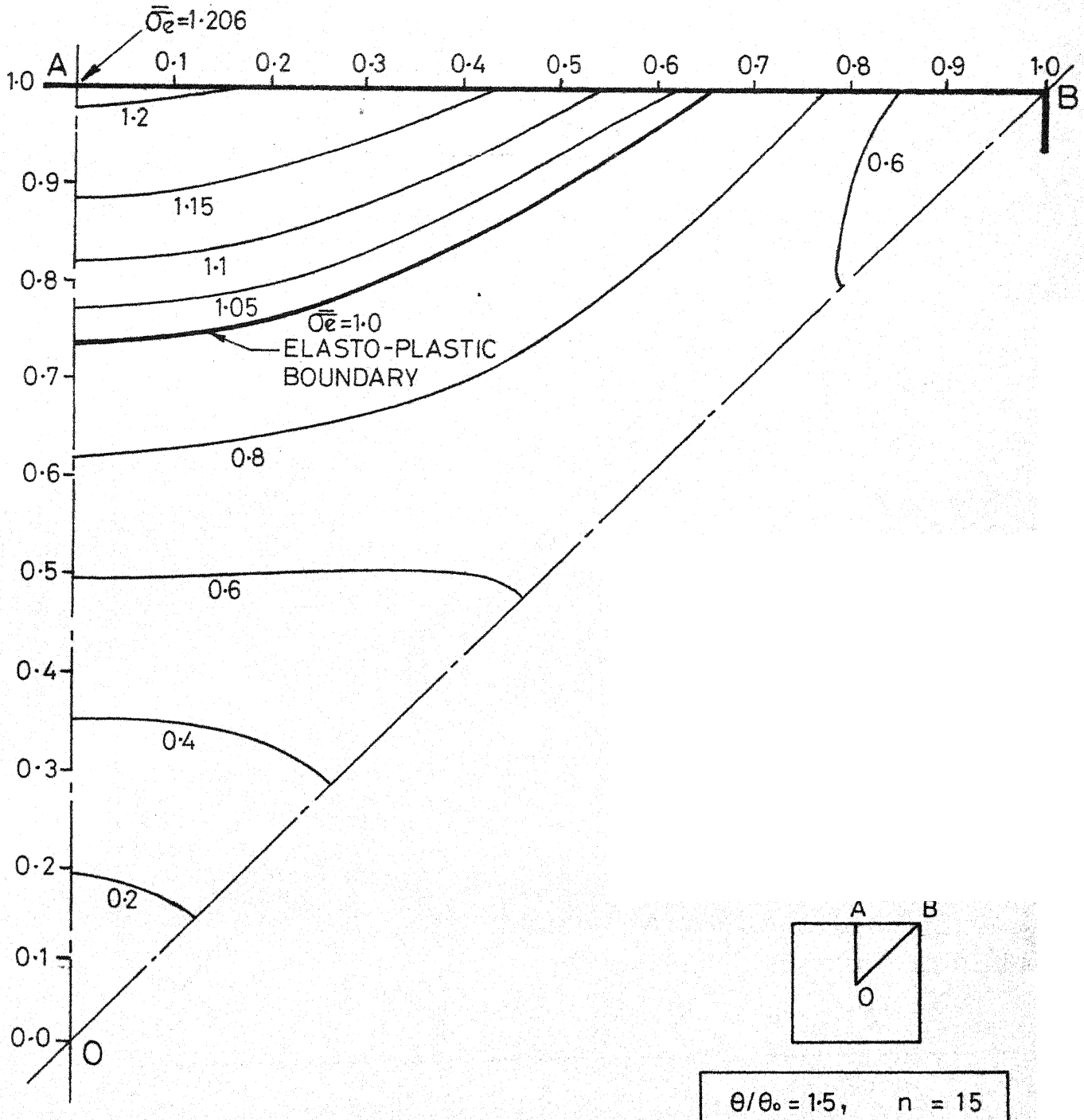

(Fig. 12) CONTOURS OF CONSTANT SHEAR-STRESS $\bar{\sigma}_e$.

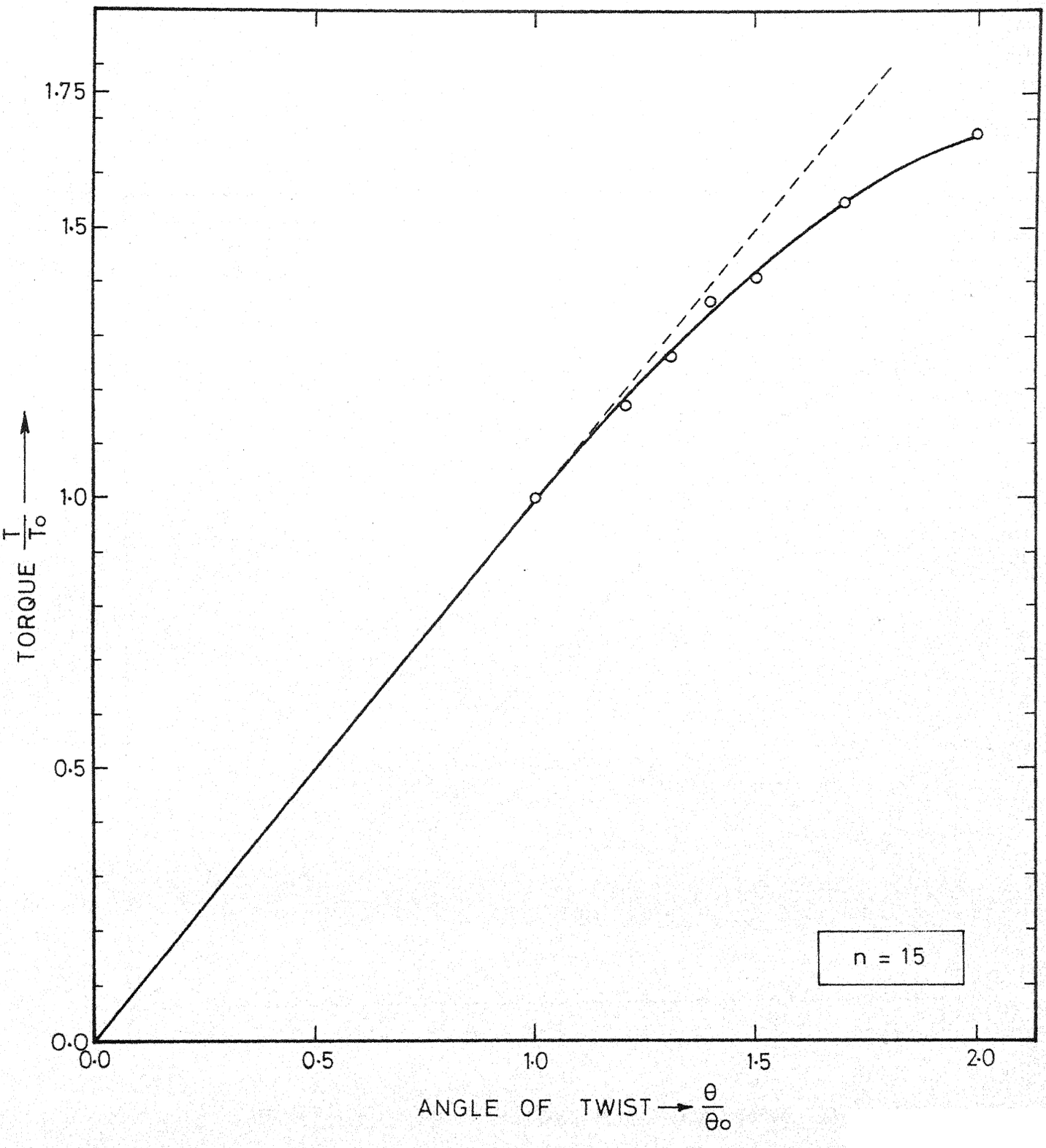

(Fig. 13) $\frac{T}{T_o}$ VS $\frac{\theta}{\theta_o}$

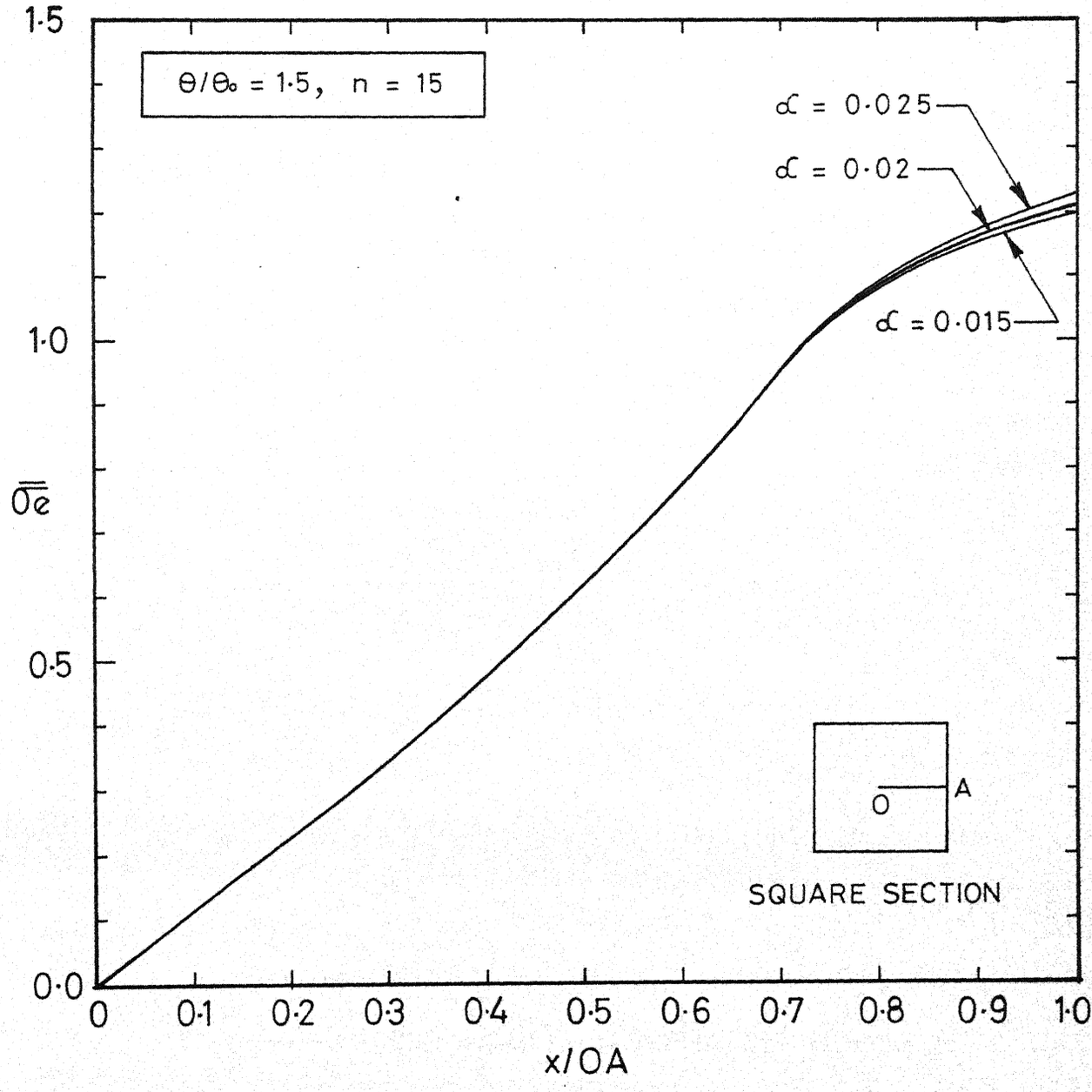

(Fig. 14) $\overline{\theta e}$ ALONG THE CENTRAL LINE OA FOR DIFFERENT VALUES OF α.

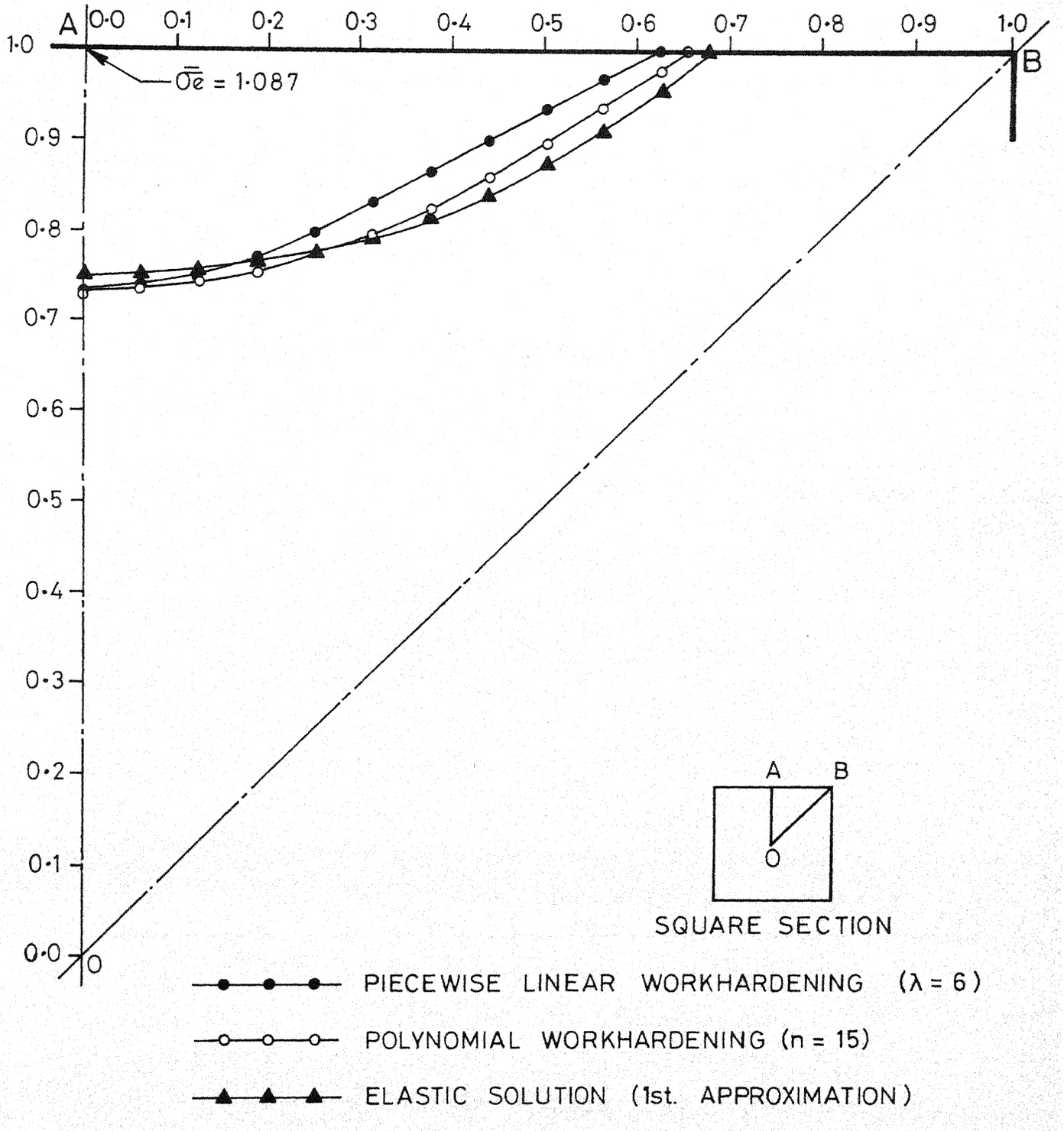

(Fig. 15) ELASTO-PLASTIC BOUNDARY FOR PIECEWISE LINEAR STRESS STRAIN CURVE.

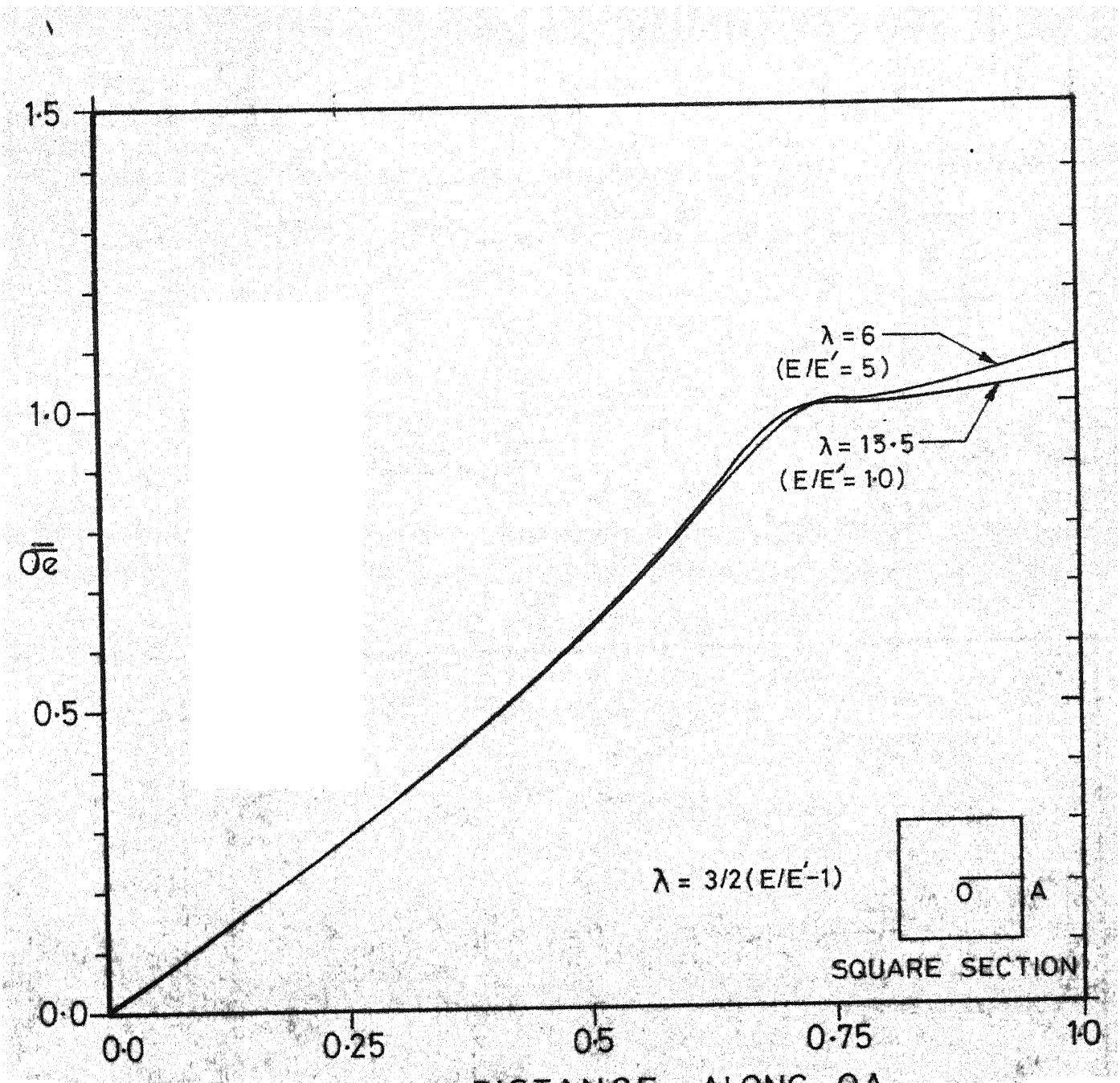

(Fig. 16) PIECE-WISE LINEAR WORKHARDENING FOR ANGLE OF TWIST $\theta/\theta_0 = 1{\cdot}5$

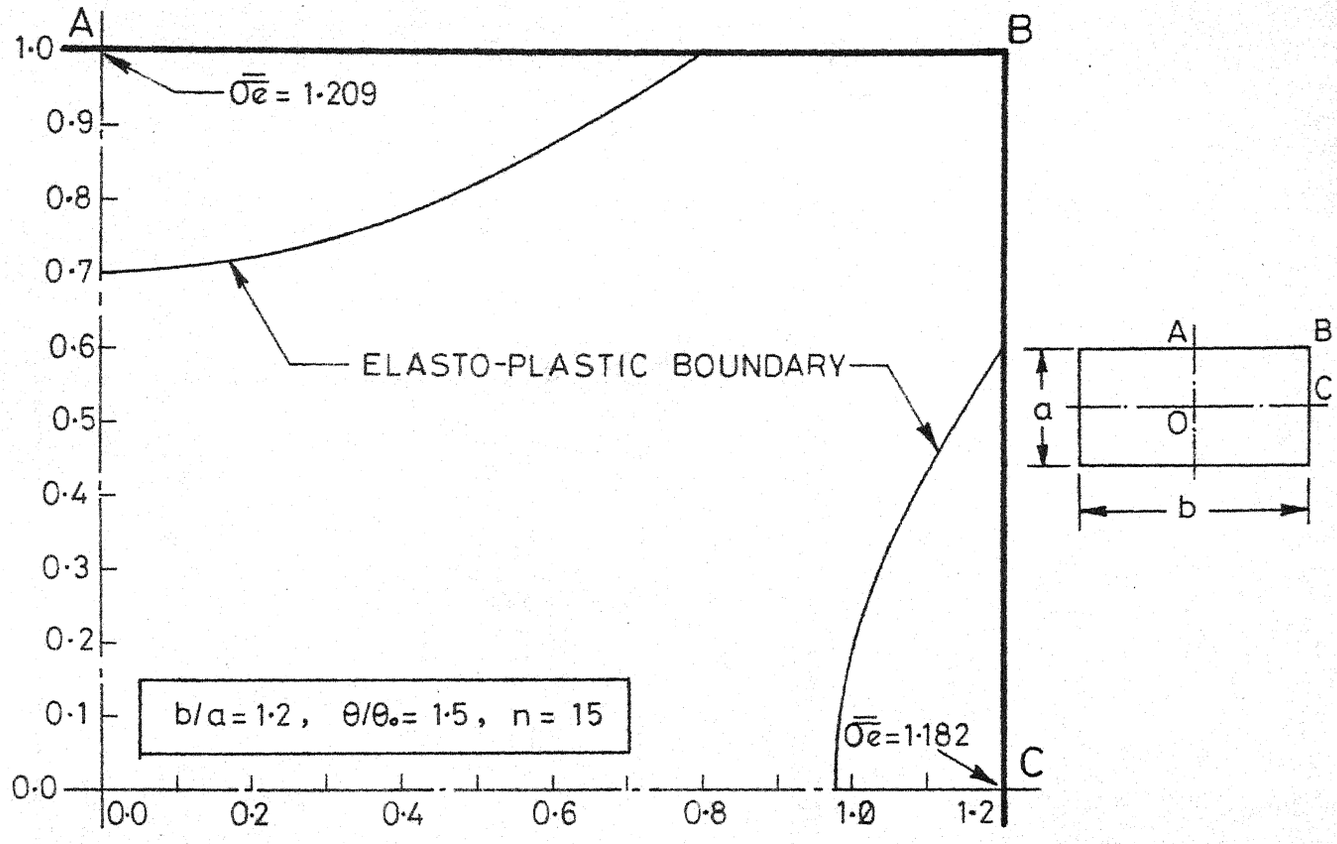

(Fig. 17a)

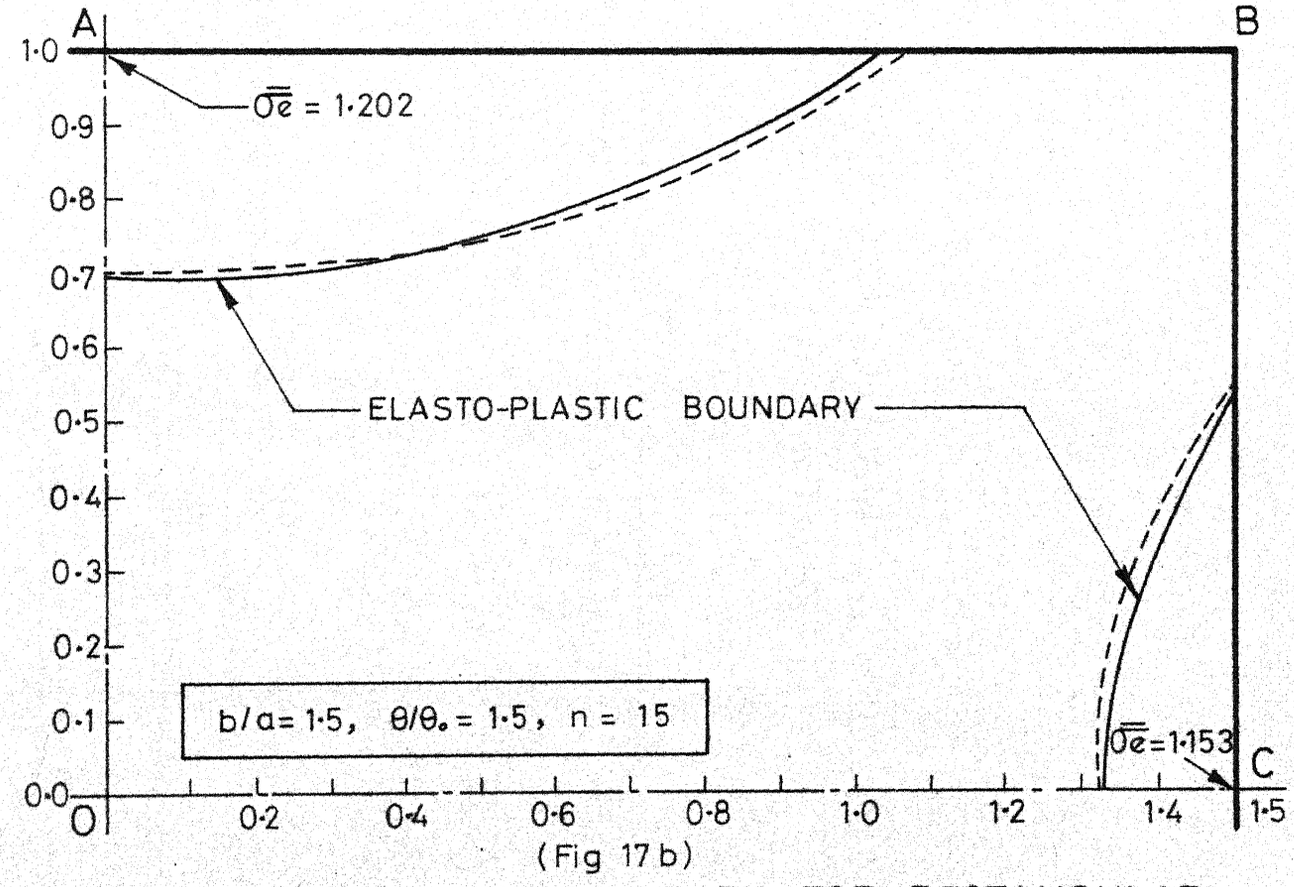

(Fig 17 b)

ELASTO-PLASTIC BOUNDARY FOR RECTANGULAR SECTIONS.

(Fig. 17 a & b)

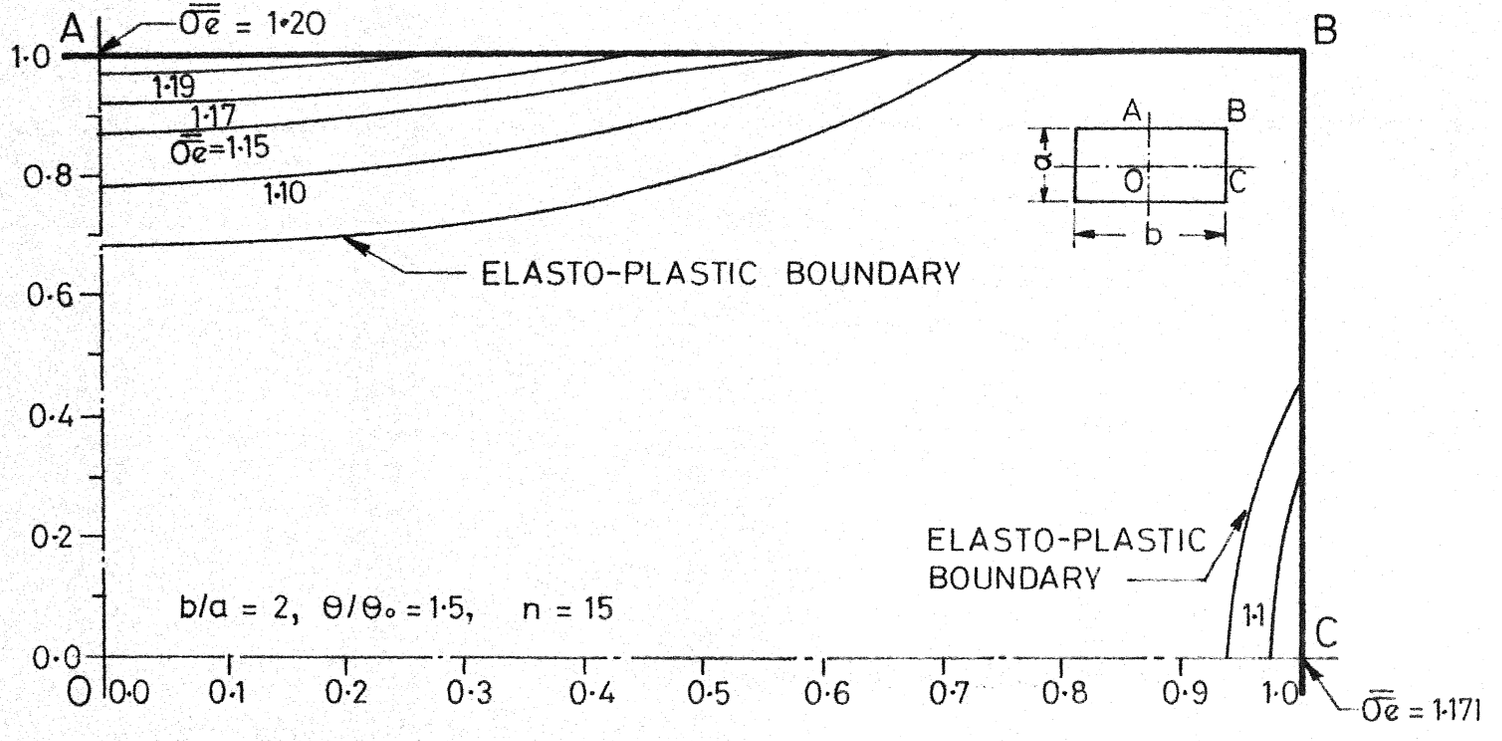

(Fig.18) CONTOUR OF SHEAR STRESS $\overline{\sigma e}$ IN THE PLASTIC REGION.

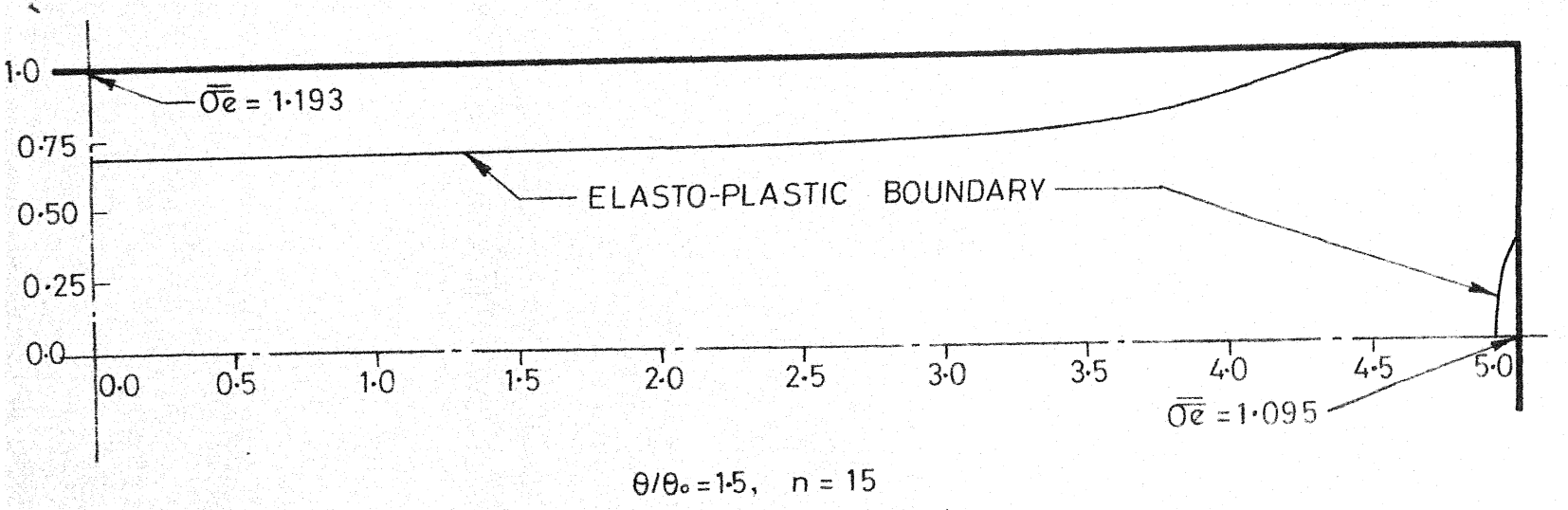

(Fig. 19) ELASTO-PLASTIC BOUNDARIES IN A RECTANGULAR SECTION b/a = 5.

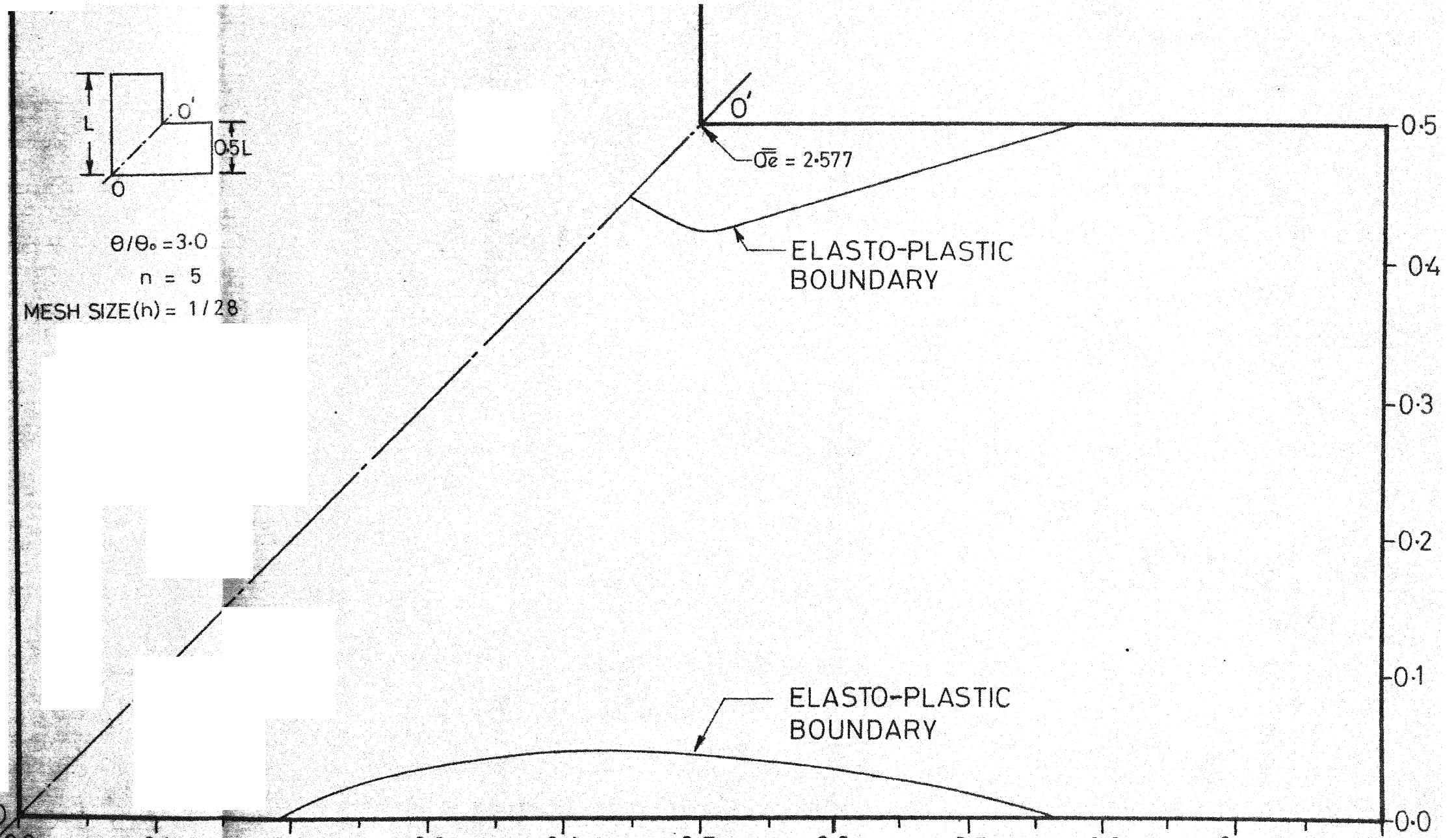

(Fig.20) ELASTO-PLASTIC BOUNDARIES IN A L-SECTION CUT OUT OF A SQUARE.

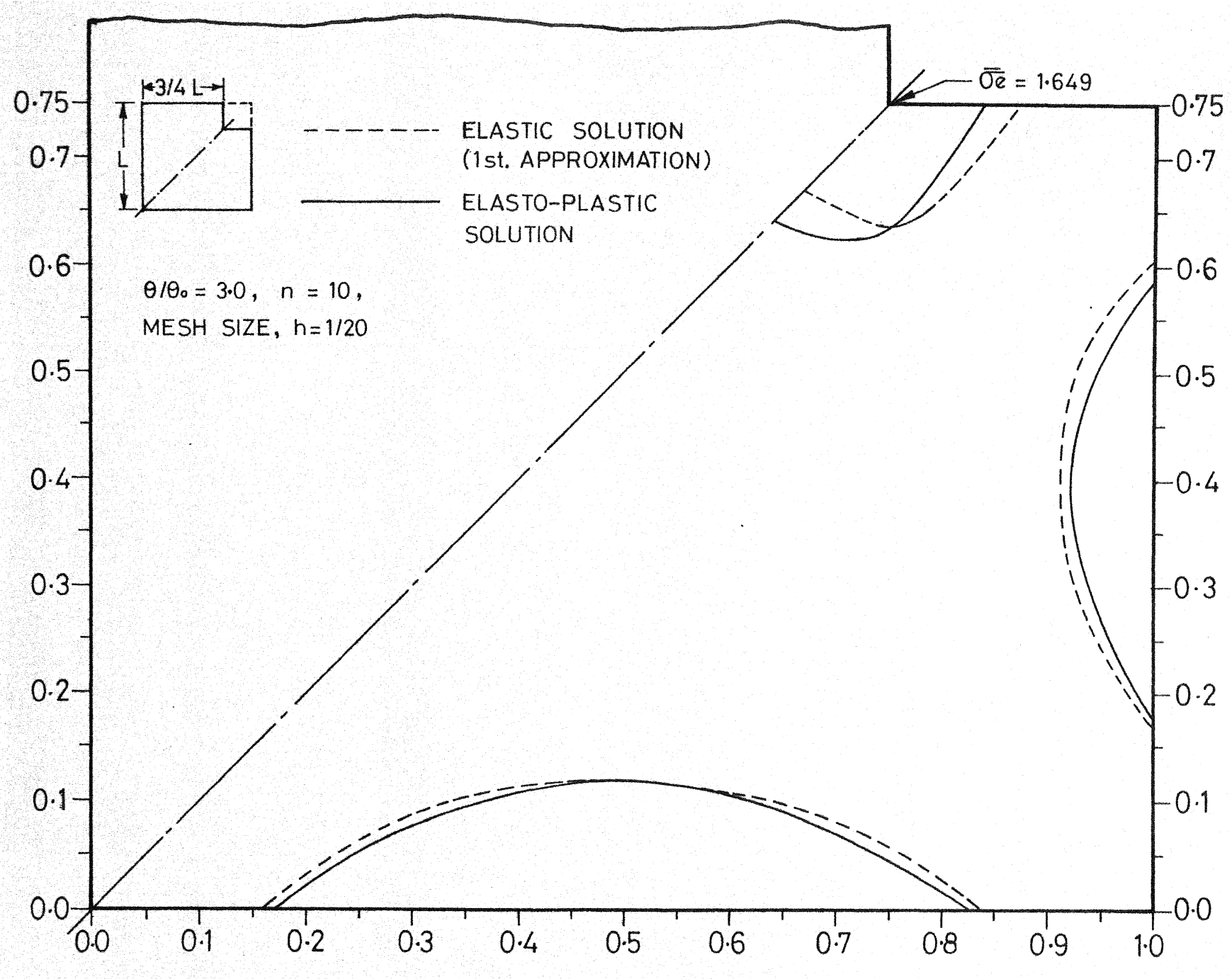

(Fig. 21) ELASTO-PLASTIC BOUNDARIES IN A L-SECTION CUT OUT OF A SQUARE.

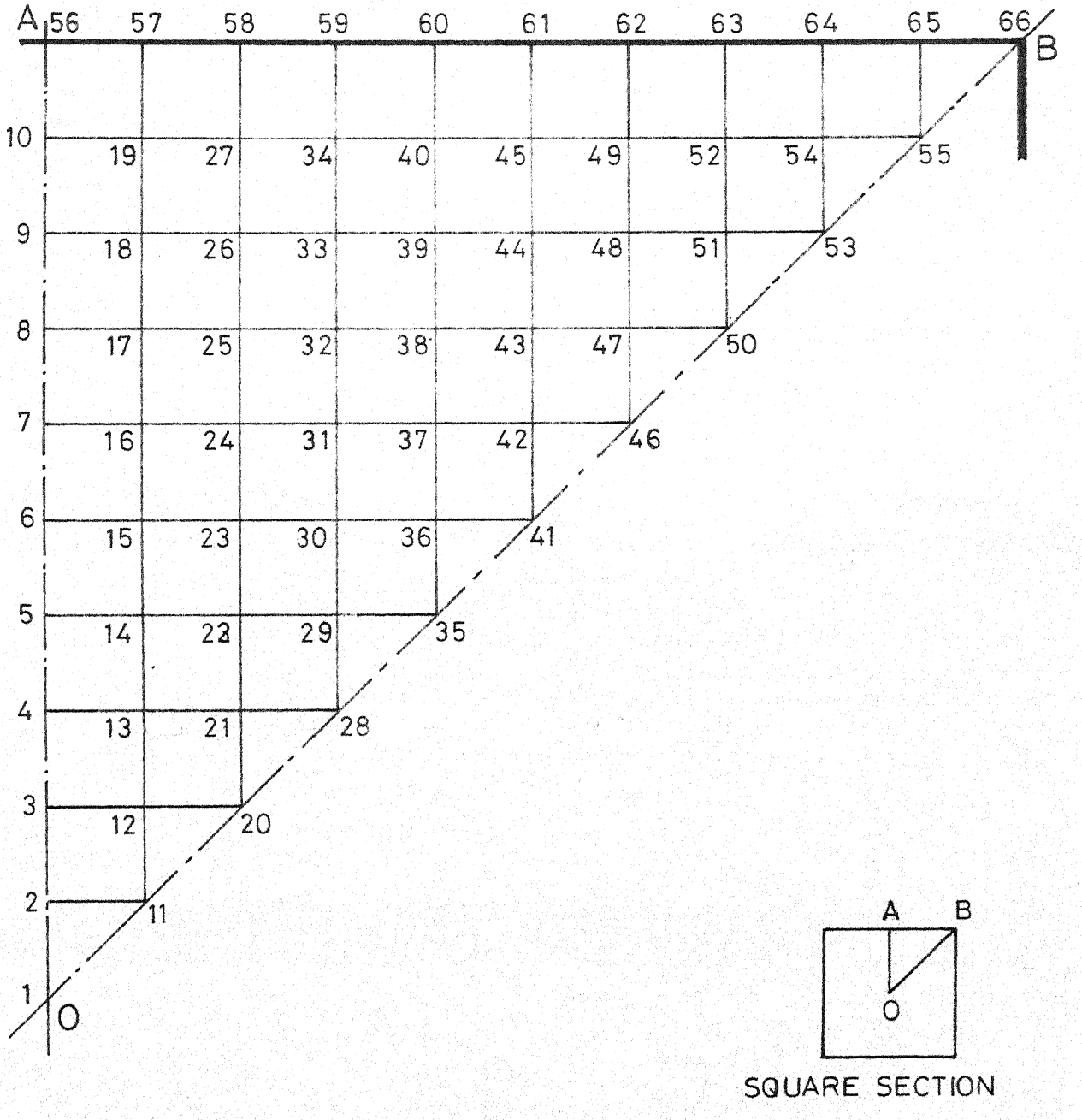

(Fig. 22) DESIGN OF THE GRID USED FOR SQUARE SECTION.

Date Due

Date	Issued to